Materials Advances

ROYAL SOCIETY OF CHEMISTRY

REVIEW

View Article Online
View Journal | View Issue

Cite this: *Mater. Adv.*, 2026, 7, 3495

Recent advancements in polyaniline-based composites for biological applications: a review

Chetna Kumari,[a] Sapana Jadoun[b] and Nirmala Kumari Jangid *[a]

Received 13th December 2025,
Accepted 23rd February 2026

DOI: 10.1039/d5ma01462j

rsc.li/materials-advances

Polyaniline, one of the most extensively studied conducting polymers, has attracted significant attention in recent years due to its unique redox properties, tunable conductivity, environmental stability, and facile synthesis. Its ability to be functionalized and combined with a wide range of nanomaterials has further expanded its utility in the biomedical field. PANI and its composites have demonstrated promising antimicrobial, antioxidant, antituberculosis, anticancer, and antimalarial activities. By adjusting various synthesis conditions and additions, its structural properties can be changed. Its electrical and reversible electrochemical characteristics make it potentially useful in several applications. Recent advances highlight that incorporating nanostructures, such as metal nanoparticles, carbon-based materials, and biopolymers, can significantly enhance the biocompatibility, sensitivity, and functionality of PANI-based frameworks. This review paper provides an overview of the latest advances in PANI-based hetero-ring derivatives and composites for biological applications.

1. Introduction

The amino groups on PANI, the length of the polymer chain, electrostatic interactions, and lower concentrations of residual low-molecular-weight byproducts are some of the factors that contribute to PANI's effective antibacterial and antifungal efficacy against particular infections. A positively charged PANI attaches to the negatively charged bacterial membrane to prevent its survival, growth, and proliferation.[1] PANI's insoluble nature in aqueous solutions extends its antibacterial action time. The reuse of PANI coatings is a significant benefit over the previously proposed antibacterial agents. In addition, adding functional groups to PANI's aromatic ring would increase the polymer's solubility in organic solvents, making it much easier to create thin films. Therefore, a high-quality coating with outstanding usability would result from combining high solubility in organic solvents with antibacterial activity.[2]

A particular class of synthetic polymers, intrinsically conducting polymers (ICPs), exhibits unique electro-optic properties. These polymers have conjugated chains with alternating single and double bonds.[3] The highly delocalised and simply polarisable π-electrons in ICPs play a crucial role in their electro-optic characteristics. Additionally, the nature of the intrinsic quasi-one-dimensional and the degree of intra- and inter-chain delocalisation of π-electrons influence the physicochemical properties of ICPs, including their structural, electrical, and optical properties.[4] In 1977, Alan Heeger, Alan MacDiarmid, and Hideki Shirakawa discovered iodine-doped polyacetylene, the first conducting polymer, and they received the Nobel Prize for this discovery in 2000. ICPs include polyfuran (PFu), polyaniline (PANI), polythiophene (PTh), polyacetylene (PAs), and polypyrrole (PPy).[3] Because of their strong response to electrical fields, these ICPs are widely used in biomedical applications, such as tissue engineering and biosensing.[5]

PANI has attracted significant interest as an ICP. PANI's unique doping/dedoping mechanism is one of the main factors contributing to its outstanding performance. Reversible doping and dedoping of PANI is possible through straightforward protonation and deprotonation without changing its backbone structure, in comparison to many ICPs that necessitate irreversible redox reactions for conductivity changes. Because of its ability to precisely adjust its conductivity, PANI is a very desirable material for biomedical devices, sensors, and actuators. Overall, PANI outperforms many other conducting polymers for various technological and biomedical applications due to its reversible doping behaviour, multiple stable oxidation states, low synthesis cost, environmental stability, tunable properties, and composite-forming ability.[6–10]

A variety of strategies have been developed, including copolymerisation with PANI derivatives, redoping with functionalised organic acids, and production of blends and nanocomposites with different materials.[10–13] Metal oxides can also bind to the PANI backbone, thereby supporting polymer stability for various applications.[14–18] These improved

[a] *Department of Chemistry, Banasthali Vidyapith, Banasthali – 304022, Rajasthan, India. E-mail: nirmalajangid.111@gmail.com, nirmalakumari@banasthali.in*
[b] *Sol-ARIS, Departamento de Química, Facultad de Ciencias, Universidad de Tarapacá, Avda. General Velásquez, 1775 Arica, Chile*

nanocomposites have wide applications in biological fields, including antibacterial,[19–25] antifungal,[26–29] antioxidant,[30–33] antituberculosis,[34,35] and anticancer[23,36–38] functions. The current review discusses the biological activities of PANI and its composites, including their biocompatibility, cytotoxicity, antioxidant, anticancer, antifungal, antituberculosis, and antibacterial properties.

2. Structure of polyaniline and its synthesis method

One of the earliest ICPs is PANI, known as "aniline black," which was found in the middle of the 19th century.[39] PANI's molecular structure may contain quinonoid, benzenoid, or both units in varying concentrations.[40] The basic structure of PANI is shown in Fig. 1,[41] where the leucoemeraldine state is formed by the benzenoid state, and hydrogen is close to the nitrogen elements. However, the pernigraniline state is formed by the quinonoid state, in which no hydrogen is attached to any nitrogen elements. The redox state of PANI is determined by the concentrations of c and d in the polymer chains.

For reduced leucoemeraldine, fully oxidised pernigraniline, and incompletely oxidised emeraldine, the optimal c : d ratios are 1 : 1, 0 : 1, and 1 : 0, respectively. The degree of doping and the synthesis technique can affect these ratios. The highly doped form of emeraldine salt exhibits conductive behaviour, while leucoemeraldine and pernigraniline are nonconductive. The most stable and non-toxic form of PANI is emeraldine base. Therefore, maintaining equilibrium between the benzenoid and quinonoid groups in the emeraldine salt is essential to achieving the proper electrochemical properties. The various redox structures of PANI, including the base and salt forms of leucoemeraldine, emeraldine, and pernigraniline, are depicted in Scheme 1.[41]

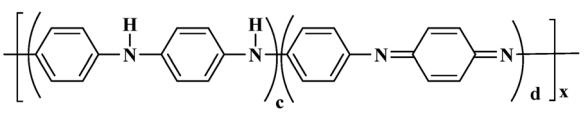

Fig. 1 Basic structure of PANI.

Both electrochemical and chemical oxidative polymerisation mechanisms in an acidic medium are used to synthesize the PANIs, as shown in Scheme 2.[1] Ammonium persulfate (APS) and potassium persulfate (KPS) are the most frequently used initiators for the chemical polymerisation of aniline.[40] The chemical method enables large-scale formation of the polymer or related composites, whereas the electrochemical method is generally used for small-scale synthesis.[42] The electrochemical techniques include co-deposition and electrode coating. The electrode coating method uses reference, working, and counter electrodes in a single-compartment cell that holds the monomer solution and the electrolyte. The co-deposition technique involves dissolving an insulating polymer host in an electrolyte solution that contains the conductive polymer's monomer.[43]

Numerous research groups have reported PANIs with varying nanostructures and characteristics because of their high surface-to-volume ratio, which improves the characteristics of their nanocomposites.[44] For high-performance applications, it is essential to optimise PANI synthesis conditions to achieve specific morphologies and sizes. PANI nanostructures, including nanogranules, nanospheres, nanorods, nanoflowers, nanofibers, and nanotubes, have been designed and synthesised using a variety of processes, including self-assembling, hetero phase interfacial, and electrochemical polymerisations.[44–51] For the synthesis of unique PANI nanostructures, numerous factors and procedures should be considered, including temperature, choice of initiator or oxidant, solvent, pH, chemical additives, electrochemistry, sonochemistry, and radiochemistry.[45] PANI was electropolymerized in an electrolyte solution of aniline and acid by applying a potential difference between the working and counter electrodes. In contrast, it is chemically polymerized in an acidic medium using a common initiator such as KPS and APS.

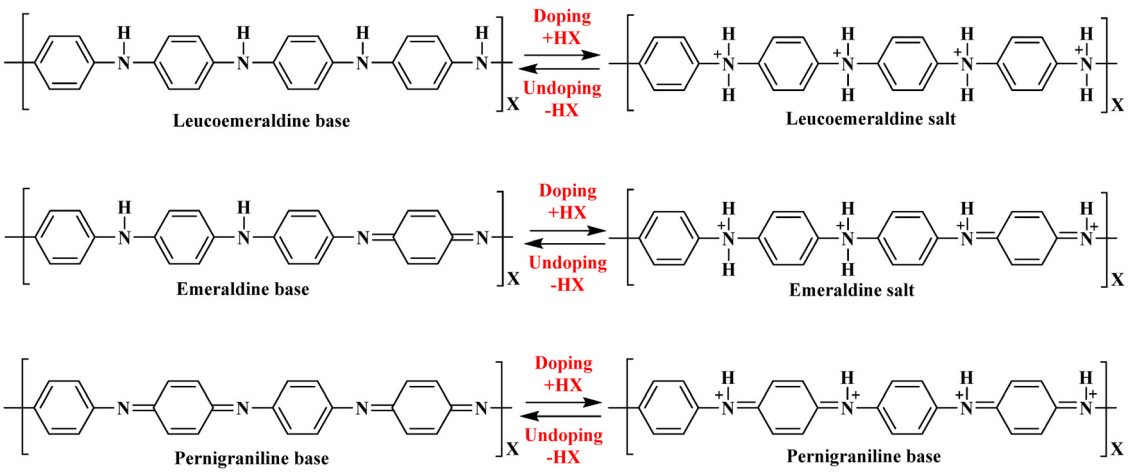

Scheme 1 Various redox structures of polyaniline.

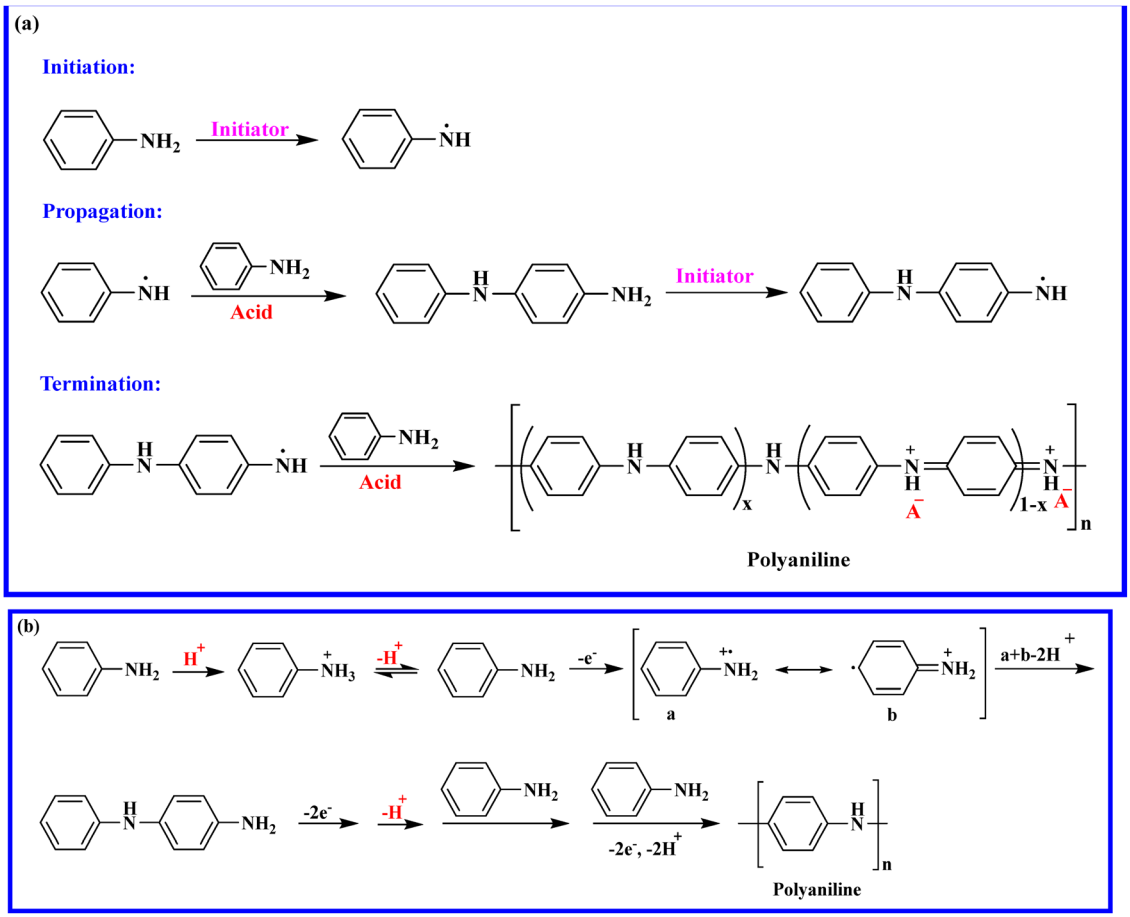

Scheme 2 (a) Chemical and (b) electrochemical polymerization mechanisms of PANI.

3. Polyaniline and its composites for biological applications

Microbial infections significantly impact human life. Therefore, extensive research has been conducted to develop novel antimicrobial drugs to combat diseases. New materials with biological qualities are constantly being discovered. In biomedical applications, polymers with antibacterial and antifungal properties are frequently used because microorganisms are developing resistance to current medications. Because of their strong biological reactivity, conducting polymers, like PANIs, are significant in biomedicine. To control microbial contamination, PANI-based drugs have been synthesized.[52,53] The antioxidant activity of PANI nanocomposites for use in biomedical applications has been the subject of a few investigations. Increasing the PANI ratio enhanced the antioxidant activity of PANI/gallic acid. This may be correlated to the PANI's ability to effectively scavenge DPPH free radicals due to its redox-active nature.[54]

3.1 Polyaniline

Jebarshia *et al.* studied PANI co-doped with various organic acids, including oxalic acid, DBSA, phthalic acid, and *Calotropis procera* latex, using a chemical oxidative polymerization method (COPM). The synthesized PANI was confirmed using various techniques, including TGA, FTIR, XRD, PL, UV, SEM, and EDX. In comparison to other composites, the DBSA-phthalic acid-doped PANI showed a maximal inhibitory zone in the antibacterial activity test against *Bacillus subtilis*. For the PANI composites, the ZI has an average value of 21–24 nm. All of the PANI composites have a minimum inhibitory concentration (MIC) of 1 mg L^{-1}. In comparison, the minimum bactericidal concentration (MBC) is 60 mg L^{-1} for PANI (DBSA-phthalic acid), 80 mg L^{-1} for PANI (DBSA-oxalic acid), and 80 mg L^{-1} for PANI (DBSA-*C. procera* latex) composites. Compared to other composites, PANI (DBSA-oxalic acid) and PANI (DBSA-*C. procera* latex), PANI (DBSA-phthalic acid) has a lower MBC value. The minimum inhibitory concentration (MIC) is the minimum amount of antibacterial agent in a culture medium that inhibits the growth of bacteria, while the minimum bactericidal concentration (MBC) is the minimum amount of an antibacterial agent needed to kill 99.9% of the bacteria. The synthesised co-doped PANI composites' potential as efficient antibacterial agents is confirmed by a larger and clearer zone of inhibition. Co-doped PANI composites increased antibacterial activity against *B. subtilis*, indicating that synthesised PANI composites may be an effective alternative to antibacterial agents for decreasing the adverse effects of harmful bacteria.[55]

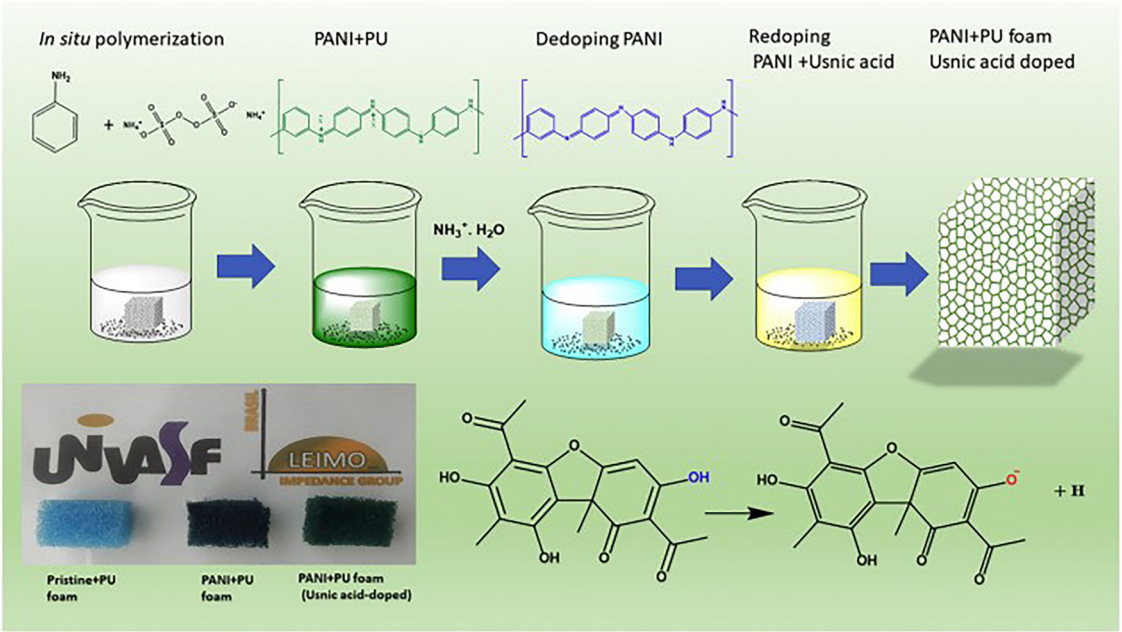

Fig. 2 *In situ* polymerization of polyaniline (reproduced with permission from ref. 56).

Santos *et al.* investigated the impact of usnic acid doping on undoped PANI, as shown in Fig. 2, by *in situ* polymerization (ISP). They achieved significant benefits, including the enhancement of the PANI bactericidal activity and the lichen derivative's antibiofilm properties. Raman, SEM, and UV spectra were used to analyse the synthesised PU and modified PU foam. The resulting material's potential as a wound dressing is enhanced by its deposition on polyurethane foam, providing a novel platform for targeting *Staphylococcus aureus* and *Escherichia coli*. According to results, both *E. coli* and *S. aureus* were able to colonise the foam surface (in both pristine and modified states) which confirms the decrease in the degree of biofilm formation on the reactor, replaced by biofilm formation on PU (pristine and modified PU foam). However, the growth of *S. aureus* is reduced by 36.75% and that of *E. coli* by 49.53% when undoped PANI is incorporated. A reduction in adhesion of 90.22% for *S. aureus* and 94% for *E. coli* is observed, indicating significant inhibition of surface bacterial growth for both Gram-positive and Gram-negative species on the foam surface. This clearly demonstrates the impact of loading usnic acid into the PANI+PU matrix. A significant strategy for developing more effective devices that leverage the favorable interactions between components is to enhance the bactericidal activity in novel composites for wound-dressing prototypes. One important factor influencing PANI's biological activity is its doping level. A potential antibiofilm prototype is produced by incorporating a sufficient level of usnic acid into polyaniline and integrating it onto polyurethane, leveraging the surface available for polymer adhesion and the combined effect of PANI doping and usnic acid's enhanced antibiofilm activity. The findings validated the composite's good activity in biofilm inhibition and reduction of the viable bacterial population; this low-cost, environmentally friendly, and effective material avoids the use of dangerous biocidals and antibiotics in favour of a natural product with a variety of uses, serving as a promising prototype for wound dressings. A low-cost substance with excellent antibiofilm agent performance is produced by the favourable combination of the highly porous surface of polyurethane, the strong bactericidal activity of PANI, and the action of usnic acid.[56]

Dhivya *et al.* investigated PANI doped with nitro chemicals, such as picric acid, 3,5-dinitrobenzoic acid, and hydrochloric acid in emeraldine salt form, which was synthesized *via* COP. By doping polyaniline chloride (PANICl), polyaniline emeraldine base (PANIEB) was synthesized. The synthesized PANI was examined by FT-IR, XRD, SEM, and UV. Doping PANI with nitro compounds increased its crystallinity. The agar well diffusion method was used to evaluate PANI's *in vitro* antibacterial activity against a variety of Gram-positive and Gram-negative bacteria, as well as the fungus *Candida albicans*. The ZI diameter and MIC values were used to evaluate the antibacterial effects. According to the test results, doped PANIs are superior to PANIEB in terms of antibacterial effectiveness. The antibacterial activity of PANI-3,5-dinitrobenzoate (PANIDN) was found to be double that of 3,5-dinitrobenzoic acid. The results indicated that PANI salts might be used for tissue implants and drug-delivery devices for slow drug release.[57]

Skopalov *et al.* synthesised the PANI using either chemical or microwave methods with two oxidising agents, KIO_3 and APS. Based on the ISO methodology and the inhibition of bioluminescence in *Photobacterium phosphoreum*, respectively, the impact on cytotoxicity and ecotoxicity was assessed. Both the synthesis process and the oxidising agent were found to have a considerable impact on biological performance. PANI's cytotoxicity and ecotoxicity were significantly enhanced by the selection of the ideal preparation conditions for PANI synthesis in comparison to PANI forms that had already been reported. It was discovered that even with 10% extract present, the $PANI^{APS}$ exhibited significant cytotoxicity. In this instance, the

cytotoxicity was not substantially impacted by the purifying process or the synthesis technique. The cytotoxicity was significantly reduced for PANI^{KIO_3}, indicating the effect of purification. The cytotoxic impact was only seen when 100% extract was present, and the greatest results were achieved for PANI$^{KIO_3\text{-}P}$ made by MW synthesis. The most promising PANI candidate for biomedical applications is prepared by an environmentally friendly technology using the KIO_3 oxidizing agent.[58]

3.1.1 Polyaniline and its hetero-ring derivatives. Kumari *et al.* investigated the one-pot synthesis of PANI and PANI–imidazole copolymer co-doped with organic and inorganic acids by COPM, as shown in Scheme 3. The produced PANI and its copolymers were characterised using a variety of methods, including conductivity tests, FTIR, XRD, SEM, TGA, and GPC. Additionally, the antibacterial activity of PANI and PANI–imidazole was evaluated by MIC, IC_{50}, and MBC against *E. coli* and *S. aureus*. PANI–imidazole (1 : 2) has a MIC of 0.50 μg mL^{-1}, an IC_{50} of 0.75 μg mL^{-1}, and an MBC of 80 μg mL^{-1}. PANI–imidazole (1 : 2) exhibits a lower MBC value against *S. aureus* and *E. coli* when compared to other copolymers and pure PANI. The synthesised co-doped PANI–imidazole copolymer exhibits strong antibacterial activity and a higher binding affinity for the bacterial enzyme than the pure PANI.[59]

Chaubisa *et al.* used ammonium persulphate and tosic acid in chemical oxidative polymerisation to create PANI–tetrazole and PANI–pyrazole composites, as shown in Schemes 4 and 5. These synthetic composites were characterised using GPC, FTIR, ^{1}H-NMR, and TGA. The PANI–pyrazole composite showed outstanding antibacterial activity against *S. aureus* and *S. pyogenes*, with an MIC of 25 μg mL^{-1}. Compared to individual PANI, the PANI–tetrazole composite demonstrated better antifungal efficacy against *Aspergillus clavatus* and *Aspergillus niger*. Furthermore, with a MIC of 0.25 μg mL^{-1}, the PANI–pyrazole and PANI–tetrazole composite demonstrated strong anti-TB action against *M. tuberculosis* H37RV. The synthesised PANI–tetrazole and PANI–pyrazole composites showed higher, positive MICs, confirming their potential as effective antibacterial, antifungal, and anti-tuberculosis agents. Overall, these results provide valuable insight into the development of new components with superior antimicrobial properties and indicate that the synthesised composite may be a viable option for use as an anti-tuberculosis agent, potentially reducing tuberculosis transmission.[60]

Kumari *et al.* used COPM to synthesize co-doped PANI and polyaniline-*co*-pyrazine (PANI-*co*-Pyr) in a single pot, as shown in Scheme 6. The structural, thermal, and electrical properties were determined using UV-visible, FTIR, TGA, viscosity, and conductivity testing. PANI-*co*-Pyr's antifungal activity against *A. niger* and *P. chrysogenum* was determined in terms of the MIC and IC_{50}, and its antibacterial property was tested against *S. aureus*, *E. coli*, *B. subtilis*, and *P. aeruginosa*. PANI's MIC and IC_{50} against *E. coli* were determined to be 0.5 and 221.56 ± 7.11 μg mL^{-1}, respectively, while PANI-*co*-Pyr (1 : 1) showed significant action against *E. coli*, with MIC and IC_{50} of 0.25 and 120.56 ± 9.01 μg mL^{-1}, respectively. PANI showed

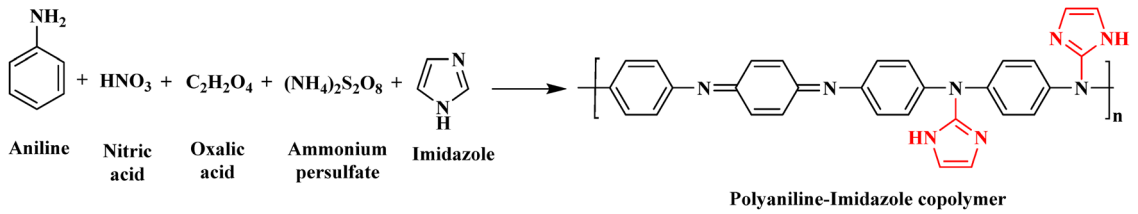

Scheme 3 One-pot synthesis of the polyaniline–imidazole copolymer.

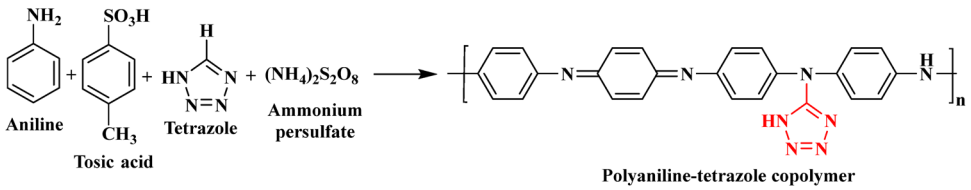

Scheme 4 Synthesis of the PANI–tetrazole copolymer.

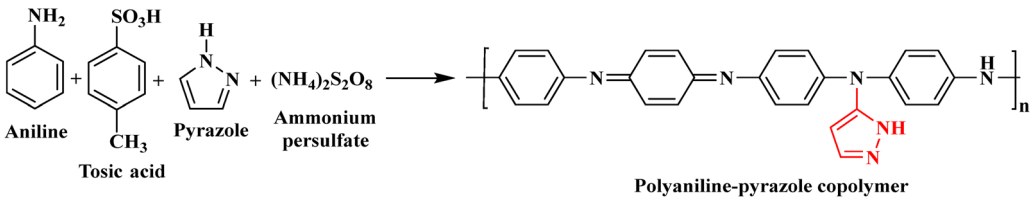

Scheme 5 Synthesis of the PANI–pyrazole copolymer.

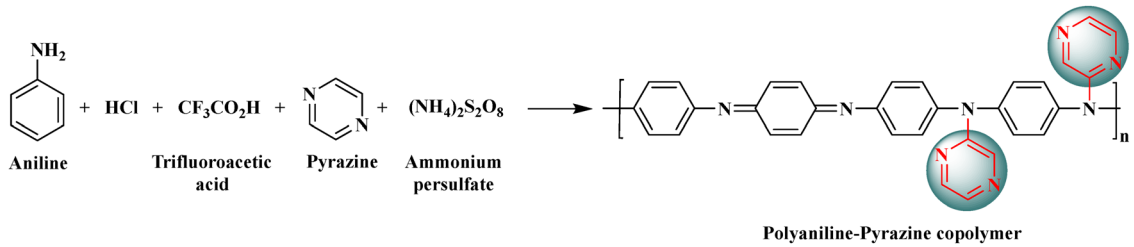

Scheme 6 One-pot synthesis of polyaniline–pyrazine copolymer.

significant efficacy against *A. niger*, with MIC and IC_{50} values of 0.5 and 332.33 ± 6.64 μg mL^{-1} for PANI and 0.25 and 200.70 ± 9.05 μg mL^{-1} for PANI-*co*-Pyr (1 : 2), respectively. The findings indicated that, compared to pure PANI, the synthesised co-doped PANI-*co*-Pyr has greater antifungal and antibacterial effects. Consequently, PANI-*co*-Pyr demonstrates strong antibacterial and antifungal action and has a greater binding affinity for fungal and bacterial strains.[61]

Chaubisa *et al.* used a chemical oxidative polymerisation technique to synthesize PANI and its copolymer with indole, using potassium persulfate as an oxidant and benzene sulfonic acid (BSA) as a dopant, as shown in Scheme 7. The TGA, GPC, FTIR, and ^{1}H-NMR methods were employed to characterise the synthesized compounds. Additionally, the copolymers' antibacterial and antifungal qualities were examined against a number of bacterial and fungal strains and determined in terms of the MIC. The PANI–indole copolymer, with an MIC of 25 μg mL^{-1}, was found to suppress *S. pyogenus* more effectively than both individual PANI and standard drugs. The PANI–indole copolymer has a MIC of 1.25 μg mL^{-1} against *M. tuberculosis* H37RV. The PANI–indole copolymer's IC_{50} for *Plasmodium falciparum* is 0.56 μg mL^{-1}. Additionally, as compared to PANI, the copolymer showed strong antimalarial and antituberculosis action. Overall, this research provides insights into the creation of novel materials with improved antimicrobial properties.[62]

3.1.2 Functionalized polyaniline. Andriianova *et al.* investigated the impact of different functional groups in the amino group of PANI and at the *ortho* position of the aromatic ring on the antibacterial activity of polymers against Gram-positive (*B. subtilis*) and Gram-negative (*P. aureofaciens*) pathogens, as shown in Scheme 8. FTIR, UV, and SEM were used to characterize the synthesized functionally substituted PANI. The antibacterial activity of functionally modified PANIs was significantly reduced when methyl, pentyl, or methoxy groups were incorporated into the *ortho* position of PANI. PANI derivatives that were altered by adding pentyl groups to the amino group are more effective as antibacterial agents than the original polymer against both Gram-positive and Gram-negative pathogens. For pure PANI, the growth inhibition zones are 43.3 mm for *P. aureofaciens* and 33.6 mm for *B. subtilis*. The polymer's bactericidal and bacteriostatic properties against Gram-positive bacteria are enhanced when a chlorine atom is present in the pentyl group. The PNClA polymer inhibits *B. subtilis* growth in a zone of 48.6 mm, whereas the zone of moderate growth is 71.0 mm. Additionally, it was discovered that N-substituted PANI derivatives exhibit both bacteriostatic and bactericidal effects on the test microorganisms. Overall, PANI was modified with N-substituted PANI derivatives, achieving a high degree of doping by varying the form and position of the substituent for use in bacterial growth suppression.[63]

Jose *et al.* investigated ternary composites of PANI/poly(aniline-*co*-3-aminobenzoic acid) (fPANI) together with TiO_2 and Ag, which exhibited improved antibacterial activity in both visible and dim light, enabling the elimination of all pathogens in 30 minutes. The synthesized PANI/fPANI–TiO_2–Ag composites were characterized by UV, FTIR, SEM, and ESR. The addition of PANI/fPANI and Ag successfully reduces the bandgap of TiO_2, making the composites visible-light-active antimicrobial compounds. By attaining complete kill in 30 minutes under visible light and demonstrating broad-spectrum action against viruses, Gram-negative bacteria, and Gram-positive bacteria, the observed antimicrobial efficacy surpasses that obtained in the laboratory setting. Compared to the PANI composites, the fPANI-containing composites demonstrated better antibacterial action against three typical microorganisms: *S. aureus*, *E. coli*, and a model virus strain called Phi X 174. Although these results pave the way for future

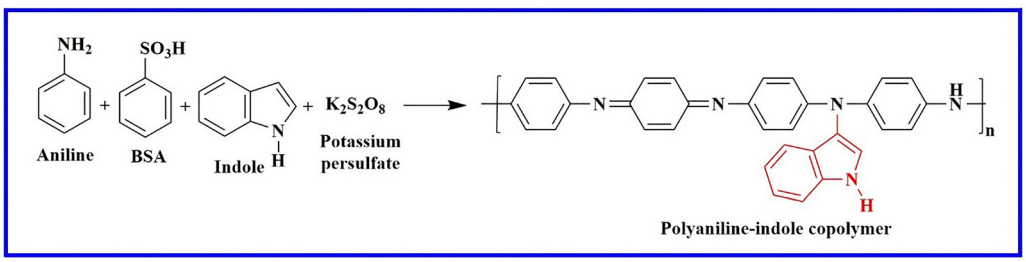

Scheme 7 Synthesis of the PANI–indole copolymer.

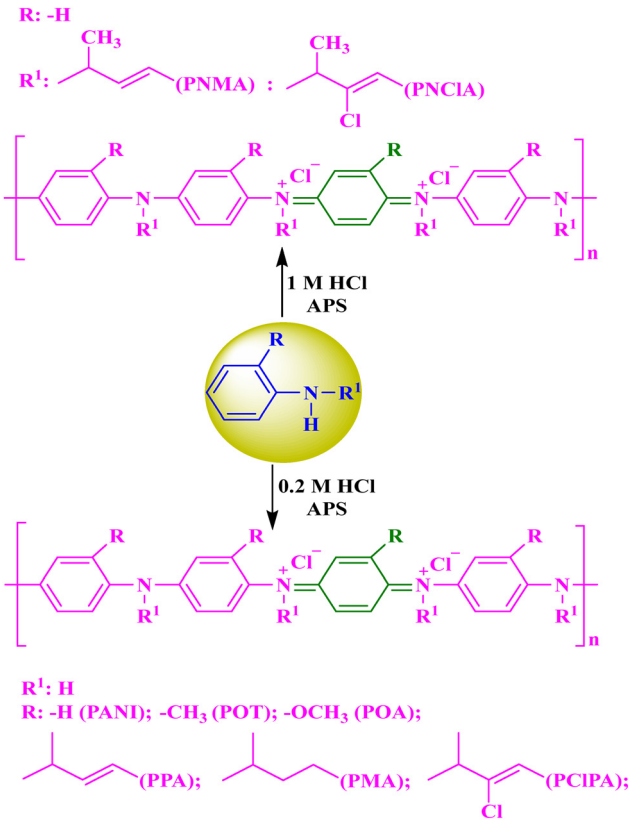

Scheme 8 Oxidative polymerization of the aniline derivatives.

developments of biocidal materials, it is important to take into account real-world constraints, especially when expanding the three-component system for use in commercial antimicrobial applications.[21]

Cai *et al.* studied bromo-substituted polyaniline (Br–PANI) using a new method, where PANI is employed as the raw material and potassium bromate and potassium bromide as the brominating reagents, as shown in Scheme 9 (Br/N = 1, A^- denotes the counter ion). The synthesized Br–PANI was characterized by TGA, FTIR, UV-visible, XPS, and SEM. It is evident from the results that Br successfully formed a chemical bond with the benzene ring of PANI. The MIC and MBC of Br–PANI are found to be 0.15 and 0.20 mg mL^{-1} against *E. coli* and *B. subtilis*, respectively. This indicates that both doped and dedoped Br–PANIs have MICs and MBCs that are significantly lower than those of doped PANI, particularly when compared with those of dedoped PANI. Furthermore, the greater the Br/N molar ratio of Br–PANI, the stronger the antibacterial properties. Br–PANI should, therefore, be a type of effective and eco-friendly antibacterial agent.[64]

Quan *et al.* studied the PANI, benzyl-substituted polyaniline (BP), and bromine-benzyl-disubstituted polyaniline (BBP), as shown in Scheme 10. The synthesized PANI, BP, and BBP were characterized by SEM, FT-IR, UV-visible, and TGA. Cardanol-based phenalkamine was used as a curing agent to prepare the bisphenol-A/poly(ethylene glycol) binary epoxy coatings (BAE/PEGE) containing BBP. BP has significant hydrophobic properties due to the substitution of benzoyl groups in the amine groups of PANI. Additionally, the strong antibacterial activity of BBP is made possible by the substitution of bromine groups in the benzene rings of PANI. With a concentration of 4 mg mL^{-1}, the sterilization ratio of the BBP suspension is 100% effective against *B. subtilis* and *E. coli*. The findings show that, in comparison to the pure bisphenol-A epoxy coating, the coatings made with PEGE and BBP perform better against bacteria and fouling. A promising method to enhance the antibacterial and antifouling properties of the prepared coated surfaces combines the fouling release effect of BAE, the fouling resistance function of PEG, and the sterilizing function of BBP. Additionally, after two weeks of immersion in the concentrated bacterial suspension and thirty days in the river, the MEBBP5% coating demonstrated outstanding antifouling ability.[65]

3.1.3 Polyaniline and its nanocomposites. Kalaiarasi *et al.* investigated pure PANI and TiO_2/PANI nanocomposites produced by the chemical oxidative method, with significantly varied TiO_2 weight percentages, as shown in Fig. 3. The produced PANI and TiO_2/PANI composites were verified using a variety of techniques, including UV, FTIR, XRD, PL, SEM, and DLS. Diazepam has been utilized extensively for its sensing activity. The disk diffusion technique was used to test the PANI/TiO_2 nanocomposite's antifungal efficacy against *Aspergillus niger* and *Aspergillus flavus*, as well as its antibacterial activity against *Klebsiella pneumoniae* and *Proteus mirabilis*. The zone of inhibition (ZI) for *Aspergillus flavus* was determined to be 11 mm, while it was 21 mm for *Klebsiella pneumoniae*. A cyclic voltammeter was used to test the improved sensitivity of the diazepam drug molecules interacting with the nanocomposites. The sensitivity of the PANI-doped TiO_2 nanocomposites was higher in comparison to pure PANI. The results showed that the metal oxide-doped PANI and TiO_2 nanocomposites enhanced polymerization and improved the sensing performance.[66]

Deshmukh *et al.* investigated the ternary silver nanoparticle-supported PANI multiwalled carbon nanotube (Ag NPs–PANI/MWCNT) nanocomposites synthesized by chemical polymerization for their antibacterial and catalytic properties, as shown in Fig. 4. UV, FTIR, XRD, TEM, XPS, and Raman spectroscopy were used to characterize the synthesized Ag NPs–PANI/MWCNT. Ag NPs–PANI/MWCNT deliver a more decisive antibacterial action against harmful bacteria. Consequently, ternary nanocom-

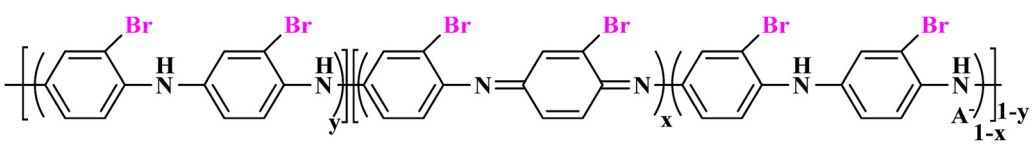

Scheme 9 Structure of Br–PANI.

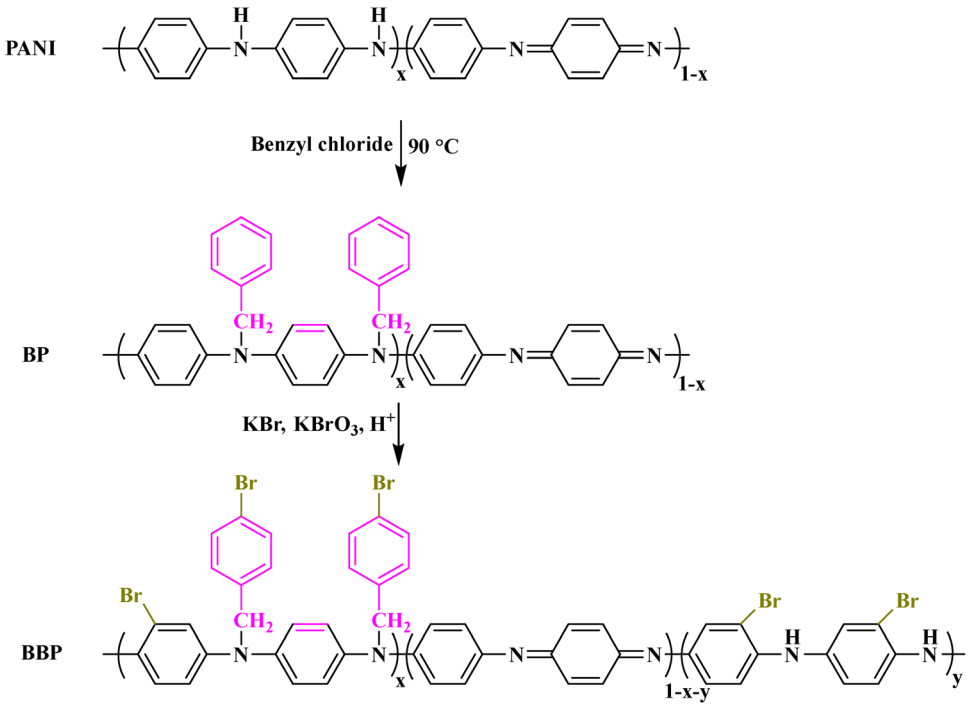

Scheme 10 Synthesis of PANI, BP, and BBP.

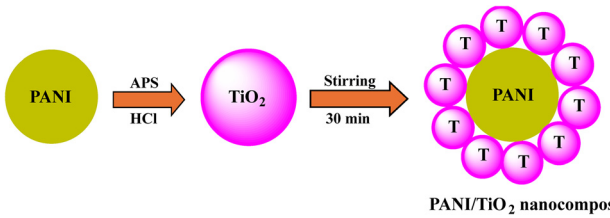

Fig. 3 Synthesis of the PANI/TiO_2 nanocomposite (reproduced with permission from ref. 66).

posites have a wide range of applications in the environmental and healthcare industries. Ternary nanocomposites have higher ZI than binary nanocomposites, according to the antibacterial investigation. Nanocomposites are a more potent antibacterial agent against both Gram-positive and Gram-negative bacteria due to their synergistic action. For the *S. aureus* and *E. coli* bacteria, the Ag NPs–PANI/MWCNT nanocomposites demonstrated 19 and 20 mm ZI at 20 μL mL^{-1}, which were greater than those of the Ag NP and Ag NPs–PANI catalysts at the same concentration, respectively. As a result, this kind of hybrid ternary nanocomposite has been investigated for use in the biomedical and catalysis fields.[67]

Ali *et al.* investigated a one-step anodization method for the synthesis of rutile mixed-phase titanium oxide layers and crystalline anatase doped with PANI. PANI has demonstrated antibacterial qualities when electropolymerized onto titanium (PANI/TiO_2). XRD, SEM, and XPS were used to characterize the synthesized polyaniline-doped titanium oxide layers. It has been demonstrated that the anodization of titanium produces crystalline oxides that, when exposed to UV light, generate reactive oxygen species (ROS). The ROS then kills bacterial cells, thereby decreasing bacterial adhesion to titanium implant surfaces. Compared with the control oxides anodized in 1 M sulfuric acid without aniline, the 0.75 M aniline oxide group also showed improved cell survival, higher hydrophilicity, and a significant decrease in bacterial adhesion. The PCA of the 1 M aniline oxide group was statistically similar to that of the 0.75 M group, while the bacterial attachment levels were more variable. According to this study, the most promising aniline oxide group for use in the future is the 0.75 M group. The cytocompatibility of PANI-doped oxides and approximately 100% cell viability were verified using MTT and live/dead assays.[68]

Maruthapandi *et al.* evaluated the antibacterial activities of CuO, TiO_2, or SiO_2 coated on PANI using a sonochemical technique for two Gram-negative pathogens: *Klebsiella pneumoniae* (KP) and *Pseudomonas aeruginosa* (PA). FTIR, SEM, and XPS were used to characterize the synthesized CuO, TiO_2, or SiO_2-coated PANI. In the absence of PANI, 220 g mL^{-1} concentrations of CuO, TiO_2, or SiO_2 showed no antibacterial activity. In contrast, after 6 h of treatment, PANI–CuO and PANI–TiO_2 (1 mg mL^{-1}, each) totally inhibited PA development, whereas PANI–SiO_2, at the same dose, did so after 12 h. PANI–SiO_2 induced less damage to KP than PANI–TiO_2, with eradication times of 12 h and 6 h, respectively. PANI–CuO had no effect on this particular microorganism. However, each PANI composite exhibits distinct antibacterial activity against these two Gram-negative bacteria. For several *E. coli* bacteria, the MIC for $CuSO_4$ is between 16 and 20 mM (1017–1271 g mL^{-1}). All of the composites firmly bind to the negative groups in bacterial cell

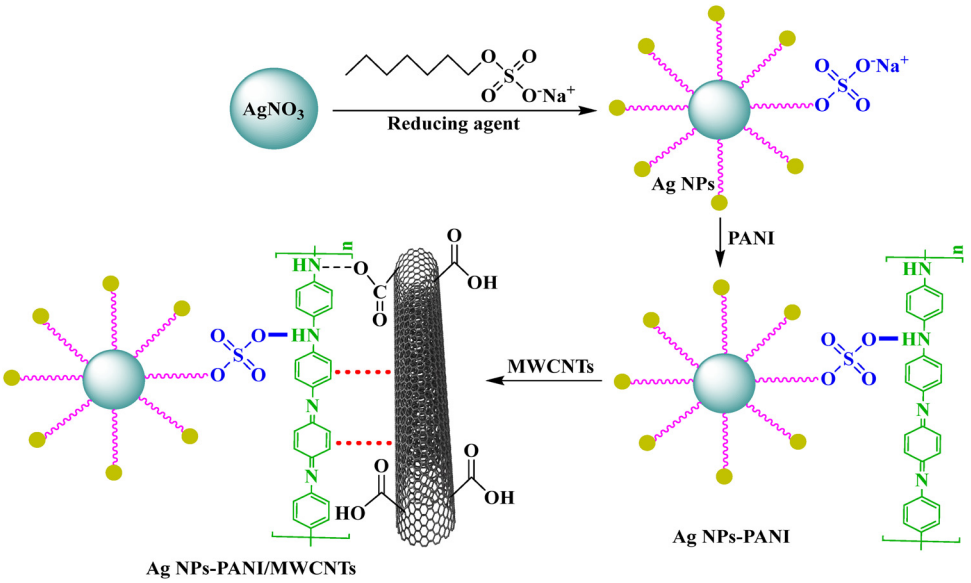

Fig. 4 Diagrammatic representation of the Ag NPs–PANI/MWCNT nanocomposites (reproduced with permission from ref. 67).

walls, interfering with their normal functions and leading to cell–wall envelope degradation and ultimately cell lysis.[69]

Alam *et al.* investigated the synthesis of a nanofiltration membrane composed of a polyphenylsulfone (PPSU) substrate with a PANI coating, as shown in Fig. 5. The PANI film served as an effective antibacterial coating and separation enhancer. The membrane shape, topography, contact angle, and zeta potential were examined using atomic force microscopy and SEM. They discussed how the PANI coating affects the membrane's surface characteristics. Significant benefits, including precisely calibrated nanometer-scale membrane holes and customized surface characteristics (*e.g.*, enhanced hydrophilicity and zeta potential), were achieved by coating the PPSU membrane with a PANI layer. The antibacterial activity of the membrane was improved by the PANI film. After incubation with *Escherichia coli* for 6 and 16 h, the bacteriostasis (B_R) values of PANI-coated PPSU membranes were 63.5% and 95.2%, respectively. After 6 and 16 h of incubation with *S. aureus*, the BR values of the

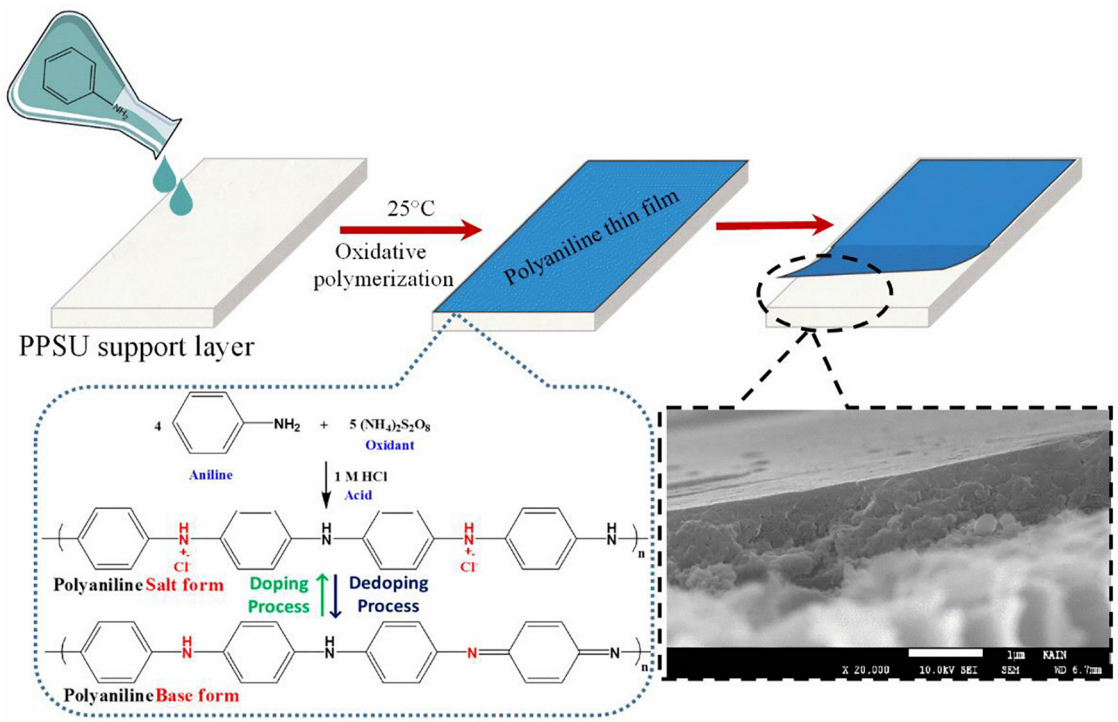

Fig. 5 Diagrammatic representation of the oxidative polymerization used to synthesize the PANI thin films (reproduced with permission from ref. 70).

PANI-coated PPSU membranes were 70.6% and 88.0%, respectively. The higher antibacterial activity of the PANI-coated PPSU membrane prevented bacterial adhesion and growth.[70]

Maruthapandi *et al.* investigated the synthesis of nitrogen-doped carbon nanodots (N@CDs) by hydrothermal processing of bovine serum albumin. After that, a PANI-N@CDs nanocomposite was prepared *via* ultrasonication. The PANI-N@CDs nanocomposite was examined using fluorescence spectra, FTIR, XPS, SEM, and TEM. Additionally, the nanocomposite demonstrated antibacterial activity against both Gram-positive and Gram-negative bacteria, including *S. aureus* and *E. coli*. Within 24 h, the PANI-N@CDs also demonstrated potent antibacterial activity against *E. coli* and *S. aureus* within 24 h. The nanocomposite's MICs for *S. aureus* and *E. coli* were 750 g mL^{-1} and 1000 g mL^{-1}, respectively. PANI-N@CDs showed improved growth-suppressing activity against *S. aureus* and *E. coli* at 1000 g mL^{-1} within 24 h. While the nanocomposite formed a complex with the bacteria and obstructed the flow of nutrients and waste products in and out of the cytosol, the release of ROS successfully destroyed cell walls and components.[71]

Falak *et al.* investigated the use of flat and honeycomb-patterned (HCP) poly-caprolactone (PCL) films to coat PANI on their surface, as shown in Fig. 6. The breath figure (BF) technique and simple solvent evaporation were used to synthesize the flat and HCP PCL films, respectively. Additionally, the impact of sulfuric acid on PANI's chemical structure and antibacterial activity was investigated. The synthesized HCP PCL films were examined using TGA, FTIR, EDX, and SEM. The film's conductivity and wettability were also analyzed. The PANI coating on the patterned surface and the chemically modified PANI both improved the film's conductivity. The antibacterial and antibiofilm activities against *S. aureus* and *E. coli* were used to determine the application characteristics. For flat PANI, HCP PANI, and H_2SO_4-treated HCP films, the antibacterial activities were 69.79%, 78.27%, and 88% against *E. coli* and 32.73%, 62.65%, and 87.97% against *S. aureus*, respectively. Similarly, *E. coli* biofilm development was decreased by about 41.62%, 63%, and 83.88% with PANI-coated flat, HCP, and H_2SO_4-treated HCP films, while *S. aureus* biofilm formation was suppressed by 17.81%, 69.83%, and 96.57%, respectively. Because of the increased PANI coating on the HCP surface, the antibacterial activity of the HCP film was greater than that of the flat PANI films. Furthermore, the HCP film's wettability may have been enhanced by sulfonation with H_2SO_4, thereby increasing its antibacterial and antibiofilm properties. Their findings demonstrated that doping and topographical modifications are easy and affordable strategies to alter the structural and functional characteristics of films. In summary, the film's antibacterial activity was as follows: HCP-SPANI > HCP-PANI > f-PANI. The greater functionalization of PANI on the HCP film, due to its comparatively large surface area, may explain the difference in antibacterial activity between the flat and HCP PANI films. Due to the altered zwitterionic surface, the sulfonated HCP-PANI film exhibited the strongest antibacterial and antibiofilm activity. As a result, a hydrophilic surface was produced, demonstrating increased antibiofilm activity and preventing bacterial adhesion.[72]

Charoensri *et al.* investigated zinc oxide nanoparticles (ZnO NPs) functionalised with PANI to enhance surface charges. A straightforward impregnation method was used to functionalise the surface of ZnO NPs with PANI. FTIR, XRD, SEM, TEM, XPS, XRD, and TGA were used to characterise the synthesised ZnO and PANI-functionalized ZnO nanoparticles. The ZnO NPs were added to a biopolymer film to enhance its antibacterial activity, and the PANI content raised their positive surface charges. The antibacterial activity of biodegradable materials is essential for combating plastic pollution and drug-resistant microorganisms. Because of their improved hydrophobicity, the bio-nanocomposite films' water permeability was reduced. Thermoplastic starch (TPS) films were treated with PANI-functionalized ZnO NPs to assess their physical characteristics and antibacterial activity against *S. aureus* and *E. coli*. Excellent antibacterial activity against *S. aureus* (72%) and *E. coli* (76%) was demonstrated by the PANI-functionalized ZnO bio-nanocomposite films. This finding implies that PANI-functionalized ZnO NPs can enhance the antibacterial activity of TPS-based bio-nanocomposite films. The significant positive charges of the bionanocomposite film interacting with the negatively charged bacterial cell walls are responsible for the excellent antibacterial activity of the CS/ZP3-functionalized ZnO bionanocomposite film against both *S. aureus* and *E. coli* bacteria. These films would be a readily available, affordable surface-charge-modification method for the synthesis of single-use antibacterial, biodegradable thermoplastic packaging.[73]

Hou *et al.* investigated $Ag_xZn_{1-x}O_{1-0.5x}$ and $Ag_{0.02}Z_{0.98}O_{0.99}$/polyaniline (AZO/PANI) nanocomposites, prepared by the *in situ* inverse microemulsion method and the citrate sol–gel method, respectively. Using XRD, TGA, SEM, TEM, FTIR, and UV methods, the produced Ag-doped ZnO/PANI nanocomposites were examined. Using the inhibition zone, MIC, and least bactericidal concentration approaches, the antibacterial activity of the samples against *S. aureus*, *E. coli*, and *C. albicans* was tested under solar radiation. The antibacterial activity of $Ag_xZn_{1-x}O_{1-0.5x}$ was superior to that of ZnO, according to the results, and it peaked at a mole ratio of 0.02 for Ag. The AZO/PANI composites demonstrated the strongest antibacterial activity at AZO mass fractions up to 60%, and they had a greater antibacterial impact than AZO alone. The sample has the best antibacterial activity against three pathogenic organisms when the *x*AZO is up to 60%; its MICs (MBCs) are 10 (25), 10 (25), and 5 (10) mg L^{-1}.[74]

The conductive polymer PANI and PANI/silver (PANI/Ag) nanocomposites were synthesized by *in situ* polymerization, as shown in Fig. 7. The drop-cast approach was used to synthesize neat PANI and PANI/Ag nanocomposite films. PANI and PANI/Ag nanocomposites were characterized using spectroscopic methods, like UV-Vis, FTIR, and photoluminescence. The Ag-doping effect or its complex formation may be the cause of the observed increases in the electrical conductivity of the nanocomposite films compared to the clean PANI. The photoluminescence intensities of the PANI/Ag

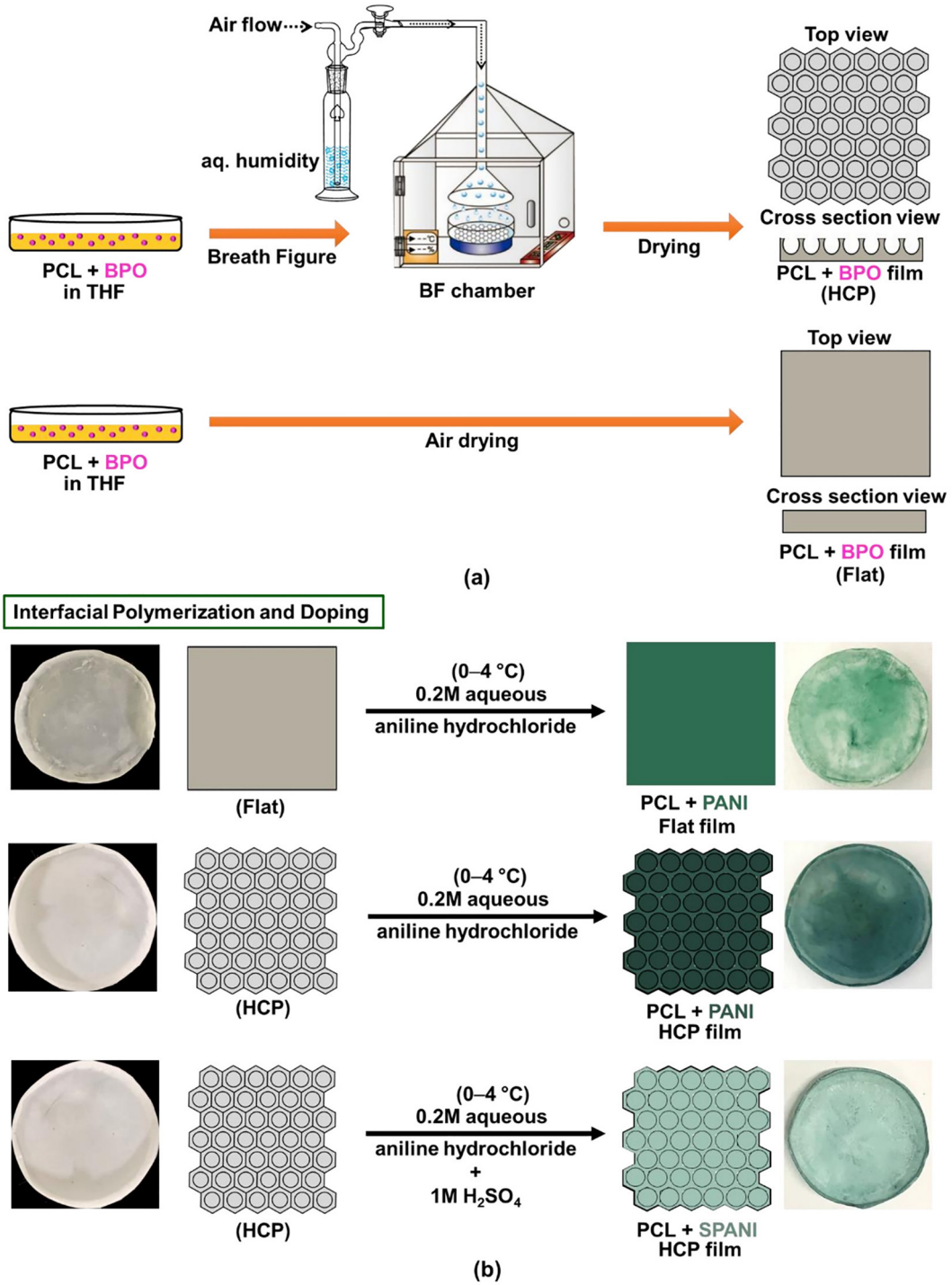

Fig. 6 (a) Synthesis of HCP (top) and flat (bottom) PCL films. (b) Interfacial polymerization of PANI at the surface of the flat (top), HCP (middle), and sulfonated HCP (bottom) films (reproduced with permission from ref. 72).

nanocomposites were greater than those of pure PANI. Using various assays, the bactericidal properties of the pure PANI and PANI/Ag nanocomposite films were examined. Microorganism viability studies revealed that after 24, 48, and 72 h, *S. aureus*, *K. pneumoniae*, *P. aeruginosa*, and *E. coli* bacteria did not form bacterial colonies. Only the 4 wt% Ag content film samples exhibited antimicrobial activity against *S. aureus* and *P. aeruginosa*, suggesting that the film with the highest antimicrobial activity was the one with the 4 wt% Ag content. In antimicrobial investigations of the films, film samples did not inhibit *E. coli* or *K. pneumoniae*.[75]

The breakdown of nanomaterials into ions is frequently the initial stage and a common cause of the toxicity of metallic nanostructures, even though the mechanisms of antimicrobial

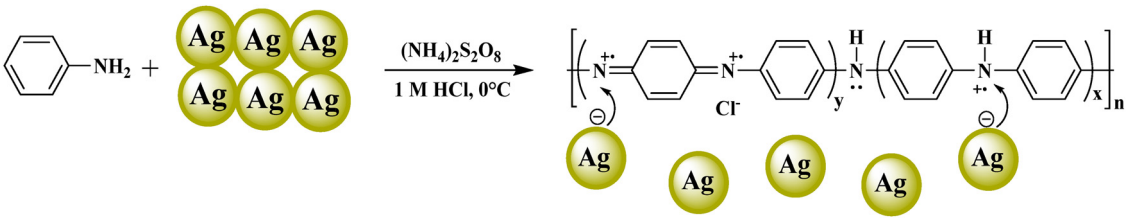

Fig. 7 *In situ* polymerisation of the PANI/silver nanocomposite (with permission from ref. 75).

activity of nanomaterials against various microbes vary with species, ions, and metals, as shown in Fig. 8[3] for a variety of nanoparticle forms. Using one or more of these methods, the bactericidal toxicity of various nanoparticle forms may be decreased. These methods encompass damage to proton efflux pumps, ROS generation, disruption of electron transport chains, and disruption of cell membranes.[3]

Boomi *et al.* investigated the synthesis of gold (Au) and gold–platinum (Au–Pt) colloids using the borohydride reduction technique with poly(*N*-vinyl-2-pyrrolidone) acting as a stabilising agent. Using a chemical method, the current study effectively synthesised and characterised pure PANI, PANI–Au nanocomposites, PANI–Au–Pt nanocomposites, and monometal (Au) and bimetal (Au–Pt) colloidal solutions. FT-IR, UV-Vis, XRD, and HR-TEM with energy-dispersive X-ray spectroscopy were used to characterise the synthesised nanocomposites. The antibacterial activity of pristine PANI, PANI–Au, and PANI–Au–Pt nanocomposites was tested against Gram-positive (*B. subtilis* and *S. aureus*) and Gram-negative (*E. coli* and *V. cholerae*) bacterial pathogens. The antibacterial activity of the PANI–Au–Pt nanocomposite against *B. subtilis* was substantial (33 ± 1.10 mm). Additionally, it was found that the MICs of the pure PANI, PANI–Au, and PANI–Au–Pt nanocomposites were 75, 50, and 25 μg mL^{-1}, respectively. Additionally, *in vitro* anticancer studies against HepG2 liver cancer cells showed that the PANI–Au–Pt nanocomposite had the maximum cytotoxicity at 21.25 μg mL^{-1}, followed by the PANI–Au nanocomposite (32 μg mL^{-1}) and pristine PANI (49 μg mL^{-1}). Overall, the current study demonstrated significant antibacterial and anticancer activity of the PANI-based materials and indicated their possible application in medicines, provided that safe and reasonably priced clinical studies are completed.[76]

Shaban *et al.* investigated PANI and Ag/PANI nanoporous composites prepared *via* oxidative polymerisation prepared *via* oxidative polymerisation. PANI nanoparticles were oxidised using APS, whereas Ag/PANI nanoporous composites were oxidised using $AgNO_3$ under artificial radiation. FTIR, XRD, SEM, and UV were used to characterise the synthesised PANI and Ag/PANI nanoporous structures. Using varying quantities of PANI NPs and Ag/PANI nanoporous composites,

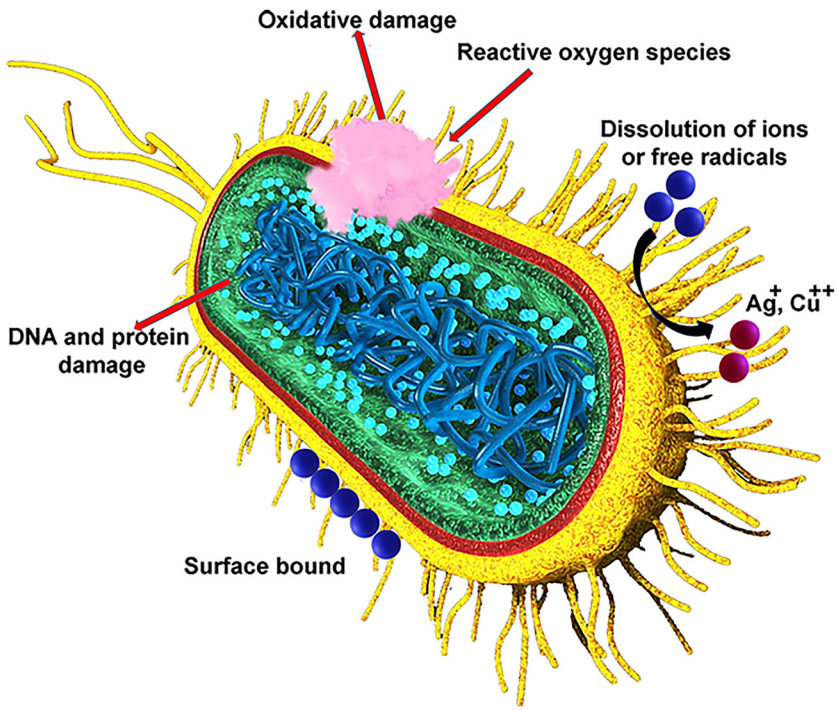

Fig. 8 An illustration of possible interactions and harmful mechanisms when manufactured nanoparticles target the cytoplasmic contents, cell wall, capsule, and cell membrane of a generic bacterium (reproduced with permission from ref. 3).

antibacterial activity tests were conducted against Gram-positive bacteria (such as *B. subtilis* and *S. aureus*) and Gram-negative bacteria (such as *Salmonella* species and *E. coli*). PANI did not exert any antibacterial effect against all pathogen strains investigated. The zone of inhibition, on the other hand, indicates that the Ag/PANI nanoporous composites had antibacterial activity. The order of the bacterial ZI is *Salmonella* species > *S. aureus* > *B. subtilis* > *E. coli*. When the concentrations of the Ag/PANI nanoporous composites were increased from 200 to 400 ppm, the ZI of all bacteria increased. However, when the dosage concentration was further increased to 600 ppm, the inhibition zones decreased. The antibacterial activity of the Ag/PANI nanoporous composite is finally described by a simpler mechanism based on electrostatic attraction.[77]

Bushra *et al.* investigated the composite material, PANI–Zr(IV) phosphoborate (PZPB), prepared by combining polyaniline and Zr(IV) phosphoborate *via* the sol–gel process, as shown in Fig. 9. Using a variety of analytical methods, including FTIR, XRD, SEM, and EDX, the PZPB composite material was described. The antibacterial efficacy of the PZPB composite material against *E. coli* was investigated. With maximal inhibition zones of 21 mm at 300 μg mL^{-1}, 16 mm at 50 μg mL^{-1}, 17 mm at 100 μg mL^{-1}, and 19 mm at 200 μg mL^{-1}, the disc diffusion method further demonstrated the inhibitory activity of the PZPB composite material.[78]

Nezhad *et al.* investigated the two-step synthesis of the colloidal PANI/ZnO/UiO-66-NH_2 nano-platform. FTIR, EDX, XRD, FESEM, UV, and TGA were used to characterize the synthesized colloidal PANI/ZnO/UiO-66-NH_2. Cytotoxicity and biological activities, including antibacterial and antioxidant properties, were evaluated. Under an 808 nm NIR laser (0.6 W cm^{-2}, 1.5 mg mL^{-1}), the nanocomposite demonstrated excellent photothermal efficiency, reaching 60 °C in 10 minutes, indicating its potential for hyperthermia-based cancer treatment. The temperature increased to 49 °C at a concentration of 0.15 mg mL^{-1}, suggesting that the photothermal treatment (PTT) is dependent on both concentration and laser intensity. NIR laser irradiation significantly reduced the viability of MCF-7 breast

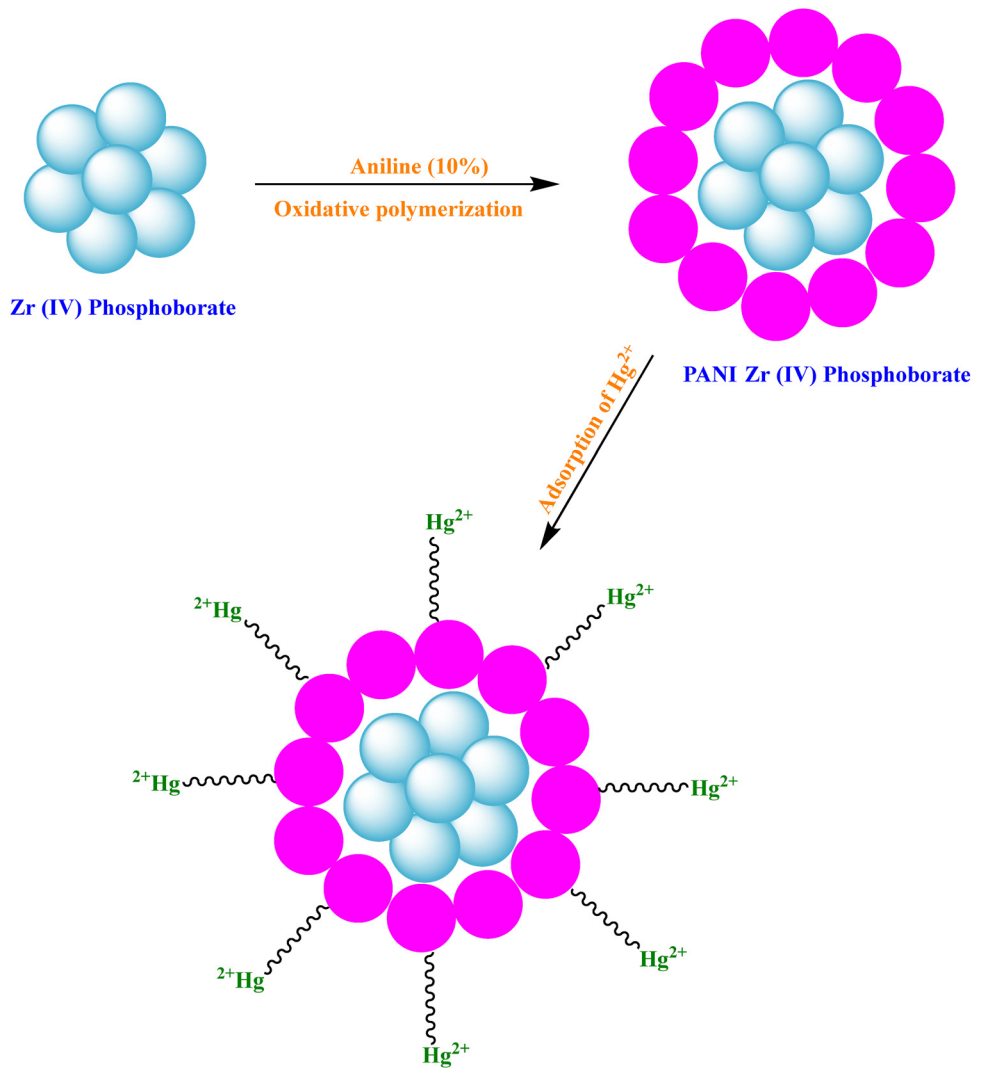

Fig. 9 Schematic for the PZPB synthesis and Hg^{2+} adsorption on PZPB (with permission from ref. 78).

cancer cells in an *in vitro* cytotoxicity study. The MTT assay demonstrated the nanocomposite's potential as a photothermal agent by confirming that combining it with laser therapy resulted in a significant reduction in cancer cell survival. Furthermore, the colloidal PANI/ZnO/UiO-66-NH_2 nanocomposite was found to have vigorous antibacterial activity against *E. coli*, *B. subtilis*, *S. enteritidis*, and *S. aureus*, as well as an antioxidant activity of 90.64%, which is comparable to the highest efficiency of UiO-66-NH_2 (94.20%). The inhibition zones for *S. enteritidis* and *E. coli* were 15 ± 0.3 mm and 13 ± 0.1 mm, respectively, indicating their dual use in PTT and antibacterial treatment. According to the MTT experiment, after 48 hours of treatment, colloidal PANI/ZnO/UiO-66-NH_2 decreased MCF-7 cell viability to 40%. After 24 h, the colloidal PANI/ZnO/UiO-66-NH_2 IC_{50} value for MCF-7 cell growth inhibition increased from 17.13 μg mL^{-1} to 32.3 μg mL^{-1}. The hemolysis tests showed 5% at 100 μg mL^{-1} and 2.5% at 10 μg mL^{-1}. Its antibacterial effectiveness was greatly enhanced when PANI and sodium carboxymethyl starch (CMS) were combined, giving it a more potent and wide-ranging antimicrobial action than the individual components. In conclusion, the PANI/ZnO/UiO-66-NH_2 nanocomposite has tremendous potential for pharmaceuticals, medical treatments, and healthcare technologies due to its superior photothermal, antioxidant, and antibacterial capabilities.[79]

Sampurnam *et al.* examined the chemically synthesized PANI/ZrO_2–Ag nanohybrids by COPM, as shown in Fig. 10. Several analytical methods, including XRD, FT-IR, DRS-UV, HR-SEM, HR-TEM, and Raman spectroscopy, were used to further analyze the synthesized PANI/ZrO_2–Ag nanohybrid. The morphological examination revealed that polymers had grown on the zirconia–Ag surface. Using the agar well diffusion assay, the antibacterial activity of the PANI/ZrO_2–Ag nanohybrid was assessed against Gram-positive and Gram-negative bacterial pathogens. The results demonstrated significant activity against *P. vulgaris*, *E. coli*, and *M. luteus*, with maximum ZI values of 17.6 ± 0.41, 16.3 ± 0.34, and 15.5 ± 0.41 mm, respectively. The DPPH radical scavenging experiment demonstrated the antioxidant properties of the PANI/ZrO_2 Ag nanohybrid (20–120 μg mL^{-1}), with the DPPH scavenging rate ranging from 7.87% ± 1.3% to 50.23% ± 1.5%. Additionally, the MTT assay was used to assess the anticancer efficacy of the PANI/ZrO_2–Ag nanohybrid against the MCF-7 breast cancer cell line. According to cytotoxicity studies, 100 μg mL^{-1} of the PANI/ZrO_2–Ag nanohybrid caused 53.3% ± 1.5% cancer cell death. The current work highlighted the antioxidant, antibacterial, and anticancer properties of the PANI/ZrO_2–Ag nanohybrid *in vitro*, which may prove to be a powerful agent for a variety of future therapeutic applications.[80]

Bogdanović *et al.* studied the synthesized PANI and Cu NPs for antimicrobial applications. The produced PANI and Cu NPs were examined using XRD, Raman, XPS, FESEM, and HRTEM. Using *E. coli*, *S. aureus*, and *Candida albicans* as microbial species, they investigated the time- and concentration-dependent antibacterial activities of the materials. After 2 h of incubation, the Cu PANI nanocomposite demonstrated effective fungicidal and bactericidal properties at concentrations <1 ppm. Atomic force microscopy showed significant cellular damage in every analyzed microbe, in addition to the quantitative analysis. Additionally, the Cu–PANI nanocomposite's MIC and MBC were lower than those of other nanocomposites. Cu–PANI at 0.2 ppm inhibits the growth of bacteria and fungi. At nanocomposite concentrations of 0.7, 1.0, and 1.0 ppm, respectively, total growth

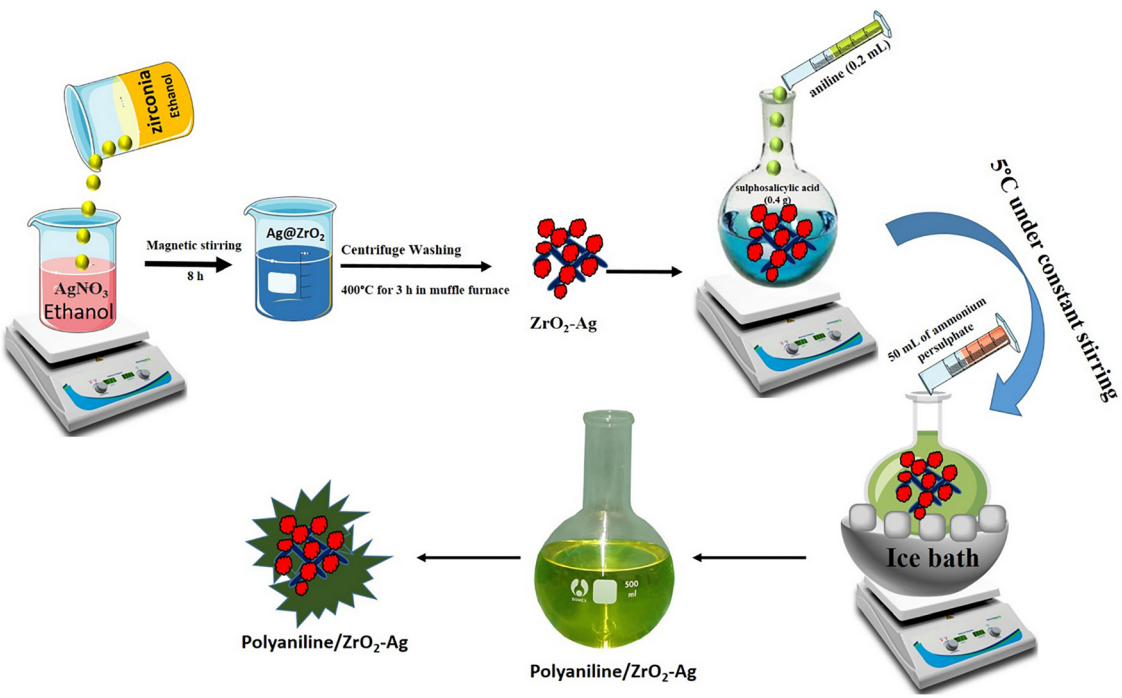

Fig. 10 Schematic of the synthesis of PANI/ZrO_2–Ag (reproduced with permission from ref. 80).

suppression (99.9% microbial reduction) was attained against *E. coli*, *S. aureus*, and *Candida albicans*. At all examined incubation times, *C. albicans* showed the least sensitivity to this concentration, and 60 minutes of exposure to Cu–PANI was insufficient to destroy the cells completely, despite a notable reduction in the proportion of fungal cells (97.9%). Only for bacterial cells could this concentration (20 ppm) be described as the MBC for a shorter incubation period (30 min) compared to the case above (0.7 and 1.0 ppm for 2 h). It has been demonstrated that using such low concentrations of the material is an effective strategy for preventing its environmental toxicity. The Cu–PANI nanocomposite is evaluated *in vitro* for its genotoxicity and impact on the oxidative state of human cells. Its release of copper ions must be quick and efficient at the biosafety threshold ($\leq$0.7 ppm) to effectively control pathogen microorganisms in polluted water before further processing. Even at low concentrations ($\leq$1 ppm), this efficacy demonstrated the intense contact between the bacteria and the nanocomposite, which prevents microbial growth and subsequent reproduction. The cytokinesis-block proliferation index (CBPI) for genotoxicity is found to be 1.46 $\pm$ 0.01 at 20 ppm. Compared to previous PANI-based nanocomposites reported in the literature, the Cu–PANI nanocomposite exhibits a remarkable and more noticeable antibacterial activity.[81]

Jayeoye *et al.* studied the synthesized gold nanoparticles/polyaniline boronic acid/sodium alginate aqueous nanocomposites ((PABA-SAL)@AuNPs), as shown in Fig. 11. The synthesized (PABA SAL)@AuNPs were examined using FTIR, XRD, FESEM, and TEM. The nanocomposite's hydrodynamic diameter was 48.6 $\pm$ 0.9 nm, and its average particle sizes were between 15 and 20 nm. The (PABA-SAL)@AuNPs showed antibacterial activity against bacterial isolates associated with seafood, with MIC and MBC values ranging from 4 to 8 μg mL^{-1}. The (PABA SAL)@AuNPs inhibited both Gram-positive and Gram-negative bacteria with different MICs ranging from 4 to 8 μg mL^{-1}. The (PABA-SAL)@AuNPs showed bactericidal activity against all tested microorganisms at an MBC of 8 μg mL^{-1}. SAL-ABA was shown to have no antibacterial activities when compared to (PABA-SAL)@AuNPs. The MICs found in this investigation were greater than the MICs of 0.3–0.5 μg mL^{-1} for AuNPs based on sodium alginate-*g*-poly(*N*, *N*-dimethylacrylamide-*co*-acrylic acid) against *Bacillus subtilis* and *V. parahaemolyticus*. However, at the maximum concentration of 6.0 μg mL^{-1}, the (PABA-SAL)@AuNPs showed a modest radical scavenging activity of 15.6%. The cytotoxicity of the synthesized (PABA-SAL)@AuNPs against Caco-2 and RAW 264.7 cells was examined at concentrations ranging from 0.39 to 50.00 μg mL^{-1}. For the produced nanocomposite, the cytotoxicity was concentration-dependent. Additionally, the (PABA-SAL)@AuNPs at 25.00 μg mL^{-1} demonstrated cell viability above 75% in the RAW 264.7 and Caco-2 cell lines. It was shown that the (PABA SAL)@AuNPs exhibited modest antioxidant activity without harming human red blood cells. Additionally, they exhibit high biocompatibility, with cell viability of at least 70% in the Caco-2 and RAW 264.7 cells. These findings support the great potential of (PABA-SAL)@AuNPs for potential biological applications.[82]

Manzoor *et al.* investigated the green synthesis of magnesium oxide (MgO) and cobalt oxide (Co_3O_4) nanoparticles using extracts from *Manilkara zapota* leaves, their surface modification with PANI (as shown in Fig. 12), and their antifungal activity against *A. niger*. Using FTIR, SEM, and XRD, the textural and structural characteristics of the modified and unmodified metal oxide NPs were assessed. By adjusting the nanoparticle dose and exposure duration, the optimal conditions for the inhibition of *Aspergillus niger* were determined. Using 24 mg of PANI/MgO and PANI/Co_3O_4 nanoparticles, respectively, maximal ZI values of 2.06 and 2.01 cm were therefore achieved at 72 h. After 48 h, the zone of inhibition against *Aspergillus niger* was 4.5 cm, and after 72 h, it had grown to 4.8 cm. The findings

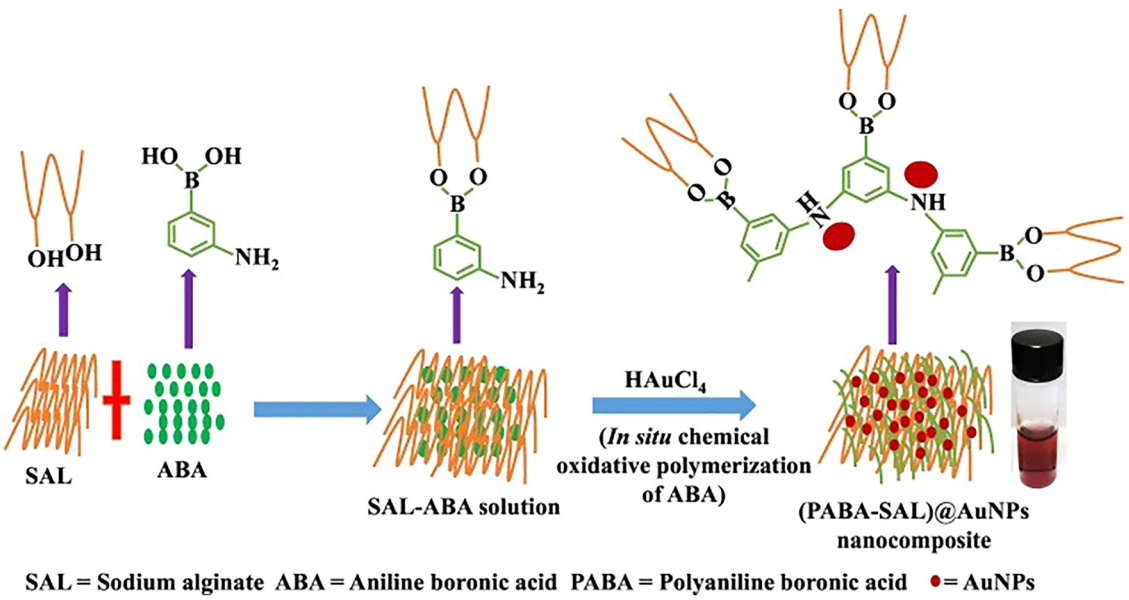

Fig. 11 Schematic of the synthesis for (PABA-SAL)@AuNP nanocomposite (reproduced with permission from ref. 82).

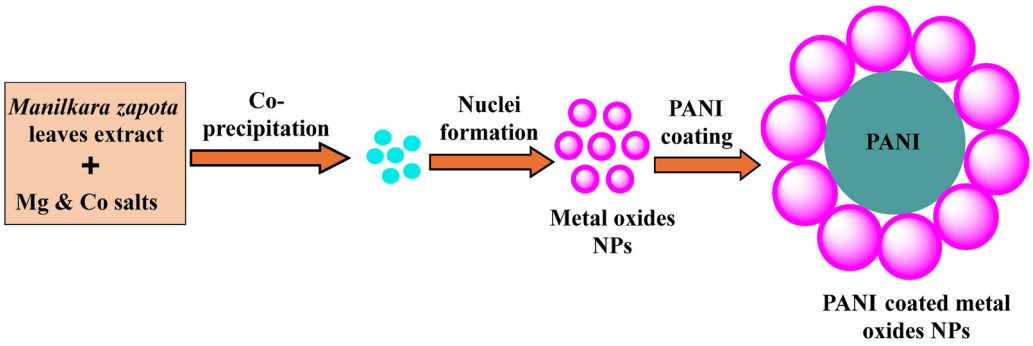

Fig. 12 Synthesis of the PANI-coated metal oxide nanoparticles (with permission from ref. 83).

show that, under ideal conditions (72 h of time exposure and 24 mM nanoparticle concentration), PANI/MgO nanoparticles outperformed PANI/Co_3O_4 nanoparticles in controlling the growth rate of *A. niger*. PANI/MgO and PANI/Co_3O_4 nanoparticles showed percentage reductions in fungal growth of 73.2% and 65.1%, respectively, which were greater than those of the unmodified metal oxide NPs (67.5% and 63.2%). Therefore, it can be concluded that the NPs examined in this study may provide an alternative to the methods currently used to prevent *Aspergillus*-caused food deterioration.[83]

3.1.4 PANI/biopolymer composites. Pasela *et al.* investigated the synthesis of PANI–chitosan (PANI–Cs) composite films *via* solution casting at varying PANI concentrations. In order to assess the viability of a PANI–Cs composite that may be used for wound dressing, this study also examined the effects of different concentrations of PANI powders on the chemical structure, morphology, and cell viability characteristics of Cs. Raman, UV, SR-FTIR, and SEM-EDX spectroscopy were used to characterize the synthesized PANI. The designed PANI–Cs composites were shown to be nontoxic in a cell viability experiment, suggesting that they may be used in biomedical applications in the future.[84]

Rehim *et al.* investigated the development of polymethyl methacrylate (PMMA)/cellulose nanocrystal (CNC) nanocomposites by physically combining different proportions of CNC with dissolved PMMA. The synthetic polyaniline-coated polymethyl methacrylate/nanocellulose composites were examined using SEM and TGA. The nanocomposite films were also coated with a layer of PANI, which imparted antioxidant properties but demonstrated negligible electrical conductivity, as verified by electrical measurements. The antioxidant capacity of the PANI-coated films was greater than that of the pure PMMA films. After 4 h, the inhibition ability increased to 45% and did not decline after 3 months of storage. Additionally, the coated nanocomposite films demonstrated effective antibacterial activity against microbes responsible for food poisoning. The results show that these modified PMMA composites may be a good option for active food packaging. However, adding the PANI

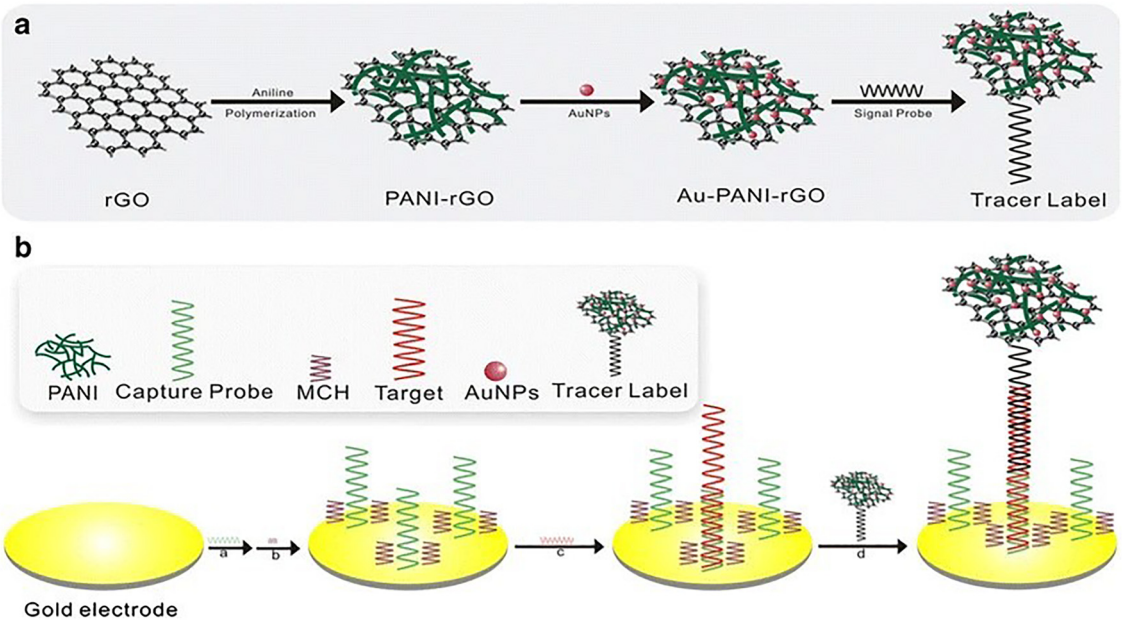

Fig. 13 Synthesis of the (a) Au-PANI-rGO, and (b) electrochemical DNA biosensor (reproduced with permission from ref. 87).

Table 1 Polyaniline and its composites used in biological applications[55–57,59–64,66–68,70–87]

S. no.	Composites	Method of synthesis	Biologica activity	Target (strains/cell lines)	Assay method	Quantitative data (MIC, IC_{50}, ZI)	Ref.
1.	PANI (DBSA-phthalic acid)	COP	Antibacterial	*B. subtilis*	Agar-well diffusion	ZI = 24.5 ± 1.5 mm	55
2.	PANI (DBSA-oxalic acid)	COP	Antibacterial	*B. subtilis*	Agar-well diffusion	ZI = 22.4 ± 1.5 mm	55
3.	PANI (DBSA-*C. procera* latex)	COP	Antibacterial	*B. subtilis*	Agar-well diffusion	ZI = 21.4 ± 1.5 mm	55
4.	PANI	ISP	Antibacterial	*E. coli*	Agar-well diffusion	$\%R_{ad}$ = 94%	56
5.	PANI–DN	COP	Antibacterial	*E. faecalis*	Agar-well diffusion	ZI = 24 mm	57
6.	PANI–DN	COP	Antifungal	*C. albicans*	Agar-well diffusion	ZI = 17 mm	57
7.	PANI–imidazole	COP	Antibacterial	*S. aureus*	Micro broth dilution	IC_{50} = 0.75 μg mL^{-1}	59
8.	PANI–tetrazole	COP	Antibacterial	*S. aureus*	Micro broth dilution	MIC = 25 μg mL^{-1}	60
9.	PANI–tetrazole	COP	Antifungal,	*A. niger*, *A. clavatus*	Micro broth dilution	MIC = 100 μg mL^{-1}	60
10.	PANI–tetrazole	COP	Antituberculosis	*M. tuberculosis* H37RV	Micro broth dilution	MIC = 0.25 μg mL^{-1}	60
11.	PANI–pyrazole	COP	Antibacterial	*S. aureus* *S. pyogenes*	Micro broth dilution	MIC = 25 μg mL^{-1}	60
12.	PANI–pyrazole	COP	Antifungal	*A. clavatus*	Micro broth dilution	MIC = 100 μg mL^{-1}	60
13.	PANI–pyrazole	COP	Antituberculosis	*M. tuberculosis* H37RV	Micro broth dilution	MIC = 0.25 μg mL^{-1}	60
14.	PANI-*co*-Pyr	COP	Antibacterial	*S. aureus*, *B. subtilis*, *E. coli*, *P. aeruginosa*	Micro broth dilution	MIC = 0.25 μg mL^{-1}	61
15.	PANI-*co*-Pyr	COP	Antifungal	*A. niger* *P. chrysogenum*	Micro broth dilution	MIC = 0.25 μg mL^{-1}	61
16.	PANI–indole	COP	Antibacterial	*S. pyogenes*	Micro broth dilution	MIC = 25 μg mL^{-1}	62
17.	PANI–indole	COP	Antifungal	*C. albicans*, *A. clavatus*	Micro broth dilution	MIC = 250 μg mL^{-1}	62
18.	PANI–indole	COP	Antituberculosis	*M. tuberculosis* H37RV	Micro broth dilution	MIC = 1.25 μg mL^{-1}	62
19	PANI–indole	COP	Antimalarial	*P. falciparum*	Micro broth dilution	IC_{50} = 0.56 μg mL^{-1}	62
20.	PANI–PNMA	COP	Antibacterial	*B. subtilis*	Disk diffusion	ZI = 35.3 ± 0.6 mm	63
21.	PANI–PNClA	COP	Antibacterial	*B. subtilis*	Disk diffusion	ZI = 48.6 ± 0.6 mm	63
22.	Br–PANI	COP	Antibacterial	*E. coli*, *B. subtilis*	Plate counting	MIC = 0.15 μg mL^{-1}	64
23.	PANI/TiO_2	COP	Antibacterial	*K. pneumoniae*	Bauer Muller Hinton agar	ZI = 21 mm	66
24.	PANI/TiO_2	COP	Antifungal	*A. flavus*	Potato dextrose agar	ZI = 11 mm	66
25.	Ag NPs–PANI	COP	Antibacterial	*E. coli*	Disc diffusion	ZI = 10 mm	67
26.	Ag NPs–PANI/MWCNT	COP	Antibacterial	*E. coli*	Disc diffusion	ZI = 20 mm	67
27.	PANI/TiO_2	Electropolymerized	Antibacterial	*S. aureus*	Tryptic soy agar	10^8 CFU per mL	68
28.	PANI/TiO_2	Electropolymerized	Cytocompatibility	Cell viability	MTT assay	100%	68
29.	PANI–PPSU	COP	Antibacterial	*E. coli*	Luria Bertani	B_R = 95.2%	70
30.	PANI-N@CDs	Ultrasonication	Antibacterial	*S. aureus*	Lysogeny broth	MIC = 750 μg mL^{-1}	71
31.	HCP-SPANI	Breath figure	Antibacterial	*E. coli*	Disk diffusion	ZI = 6.44 ± 0.27 mm	72
32.	HCP-SPANI	Breath figure	antibiofilm	*S. aureus*	Crystal violet assay	96.57%	72
33.	PANI–ZnO NPs	Impregnation	Antibacterial	*E. coli*	Agar disc diffusion	ZI = 12.40 ± 0.46 mm, 76.15%	73
34.	AZO/PANI	*In situ* inverse microemulsion	Antibacterial	*S. aureus*	Beef protein	ZI = 26.5 mm	74
35.	AZO/PANI	*In situ* inverse microemulsion	Antifungal	*C. albicans*	Sabouraud glucose agar	ZI = 28.8 mm	74
36.	PANI/Ag	ISP	Antibacterial	*S. aureus*	Muller Hinton broth	ZI = 14 mm	75
37.	PANI–Au	COP	Antibacterial	*B. subtilis*	Agar-well diffusion	ZI = 31 ± 0.45 mm	76
38.	PANI–Au	COP	Anticancer	HepG2 liver cancer cells	MTT	IC_{50} = 32 μg mL^{-1}	76
39.	PANI–Au/Pt	COP	Antibacterial	*B. subtilis*	Agar-well diffusion	ZI = 33 ± 1.10 mm	76
40.	PANI–Au/Pt	COP	Anticancer	HepG2 liver cancer cells	MTT	IC_{50} = 21.25 μg mL^{-1}	76
41.	Ag/PANI	COP	Antibacterial	*Salmonella* sp.	Classical diffusion	ZI = 22.5 mm	77
42.	PZPB	COP	Antibacterial	*E. coli*	Disc diffusion	ZI = 21 mm	78
43.	PANI/ZnO/UiO-66-NH_2	Sonication	Antibacterial	*B. subtilis*, *S. enteritidis*	Kirby-Bauer	ZI = 13 ± 0.2 mm	79
44.	PANI/ZnO/UiO-66-NH_2	Sonication	Antioxidant	—	DPPH radical scavenging	IC_{50} = 25 μg mL^{-1}	79
45.	PANI/ZnO/UiO-66-NH_2	Sonication	Anticancer	Breast cancer cell line (MCF-7)	MTT	IC_{50} = 17.13 μg mL^{-1} (24 h), 32.3 μg mL^{-1} (48 h)	79
46.	PANI/ZnO/UiO-66-NH_2	Sonication	Hemolysis	Red blood cells	Hemolysis	2.5%	79

Table 1 (*continued*)

S. no.	Composites	Method of synthesis	Biologica activity	Target (strains/cell lines)	Assay method	Quantitative data (MIC, IC_{50}, ZI)	Ref.
47.	PANI/ZrO_2–Ag	COP	Antibacterial	*P. vulgaris*	Agar-well diffusion	ZI = 17.6 ± 0.41 mm	80
48.	PANI/ZrO_2–Ag	COP	Antioxidant	—	DPPH radical scavenging	7.87% ± 1.3% to 50.23% ± 1.5%	80
49.	PANI/ZrO_2–Ag	COP	Anticancer	Breast cancer cell line (MCF-7)	MTT	53.3% ± 1.5%	80
50.	PANI–Cu NPs	COP	Antibacterial	*E. coli*, *S. aureus*	Serial dilution	99.9%	81
51.	PANI–Cu NPs	COP	Antifungal	*C. albicans*	Serial dilution	99.9%	81
52.	PANI–Cu NPs	COP	Genotoxicity	Human cells	Micronucleus	CBPI = 1.46 ± 0.01	81
53.	PANI–Cu NPs	COP	Cellular oxidative status	Oxidative stress	Thiobarbituric	0.78 ± 0.10	81
54.	PABA-SAL@ AuNPs	COP	Antibacterial	*P. aeruginosa*, *V. parahaemolyticus*	Micro broth dilution	MIC = 4 μg mL^{-1}	82
55.	PABA-SAL@ AuNPs	COP	Antioxidant	—	ABTS radical scavenging	15.6%	82
56.	PABA-SAL@ AuNPs	COP	Hemolytic effect	Red blood cells	Hemolysis	Below 1%	82
57.	PABA-SAL@ AuNPs	COP	Cytotoxicity	Cell lines (Caco-2, RAW 264.7)	MTT	75%	82
58.	PANI/MgO	COP	Antifungal	*A. niger*	Well-diffusion	ZI = 2.16 cm	83
59.	PANI/Co_3O_4	COP	Antifungal	*A. niger*	Well-diffusion	ZI = 2.01 cm	83
60.	PANI–Cs	Solution casting	Healing wounds	Cytocompatibility	Cell viability assay trypan blue assay	94.93% ± 1.5%	84
61.	PANI–PMMA/ CNC	Soaking	Antibacterial	*B. cereus* *S. typhimurium*	—	25%	85
62.	PANI–PMMA/ CNC	Soaking	Antioxidant	—	DPPH radical scavenging	45%	85
63.	CS PANI/Ch–AgNP	ISP	Antibacterial	*E. coli* *S. aureus*	Serial dilution	MBC = 1.0 wt%	86
64.	MW PANI/Ch–AgNP	ISP	Antibacterial	*E. coli*	Serial dilution	MBC = 0.25 wt%	86
65.	PANI–rGO	*In situ* reduction	Antituberculosis	IS6110 DNA fragment of *M. tuberculosis*	Affinity column	0.1 pM to 10 nM	87

layer to the films conferred them with antibacterial and antioxidant properties against foodborne microbes. As a result, PANI-coated PMMA/CNC composite sheets may hold great application promise for active food packaging technologies.[85]

Gizdavic-Nikolaidis *et al.* studied the antibacterial polyaniline/chitosan–silver nanoparticle (PANI/Ch–AgNP) composites at room temperature utilizing an environmentally friendly enhanced microwave (MW) technique. Aniline was chemically polymerized *in situ* using potassium iodate (KIO_3) as an oxidizing agent. The synthesized PANI/Ch–AgNP were characterized using FTIR, DLS, SEM, EDS, and XPS. AgNPs affected the aniline polymerization in the presence of the Ch biopolymer in the PANI-based composite. According to a comparison of the physical, morphological, and antibacterial characteristics of the PANI/Ch–AgNP samples synthesized using the improved MW approach and classical chemical synthesis (CS). The MBC of CS PANI/Ch–AgNP was found to be 1.0 wt% against *E. coli* and *S. aureus*, respectively, by the serial dilution method. Additionally, the MBCs of MW PANI/Ch–AgNP were found to be 0.25 and 2.0 wt% against *E. coli* and *S. aureus*, respectively. The bactericidal efficiency of all PANI/Ch–AgNP composites against both bacterial species was superior to that of any of the Chs or PANI control samples.[86]

3.1.5 PANI/graphene composites. The PANI–reduced graphene oxide (PANI–rGO) nanocomposite was investigated by Chen *et al.* as a redox nanoprobe in a voltammetric DNA biosensor for MTB, as shown in Fig. 13. Developed a DNA biosensor to identify a specific DNA sequence of *Mycobacterium tuberculosis* (MTB). The voltammetric signal was generated using a redox nanoprobe comprising a PANI–rGO composite with good electrochemical activity. FESEM and electrochemical analysis were used to characterize the produced PANI–rGO. Gold nanoparticles (AuNPs) were used to adorn the composite, and the tracer label was created by immobilizing the signal probe. The voltammetric signal produced by the PANI–rGO redox probe is clearly visible following the hybridization of the target DNA with the tracer label. The biosensor has a detection limit of 50 fM (at a S/N ratio of 3) and can detect the IS6110 DNA sequence of MTB over the concentration range of 0.1 pM to 10 nM. Additionally, the biosensor lacks mismatch recognition and is extremely specific. It was used to identify denatured PCR products in clinical samples, such as sputum, and the results matched those of gel electrophoresis. For the identification of MTB and, if suitable molecular markers are available, other infections, this test offers a flexible and effective tool. In summary, the current work has successfully developed an electrochemical DNA biosensor and demonstrated its use for detecting MTB. The electrochemical reaction of the redox nanoprobe (PANI–rGO) with DPV measurements makes it simple to determine the quantity of target DNA. The

biosensor's sensitivity is significantly enhanced by rGO's large surface area, which also improves the electrochemical signal and enhances PANI's immobilization. The electrochemical biosensor performs exceptionally well for evaluating clinical samples and can detect the specific IS6110 DNA fragment at the femto-
mole level. Additionally, by altering the matching sequences of the capture probe and the signal probe, this technique offers a flexible tool for identifying other infections with specific nucleic acid sequences, which may hold significant promise for accurate clinical diagnosis.[87] PANI and their composites, which are used in biological applications, are summarized in Table 1.[55–57,59–64,66–68,70–87]

4. Limitations and future outlook

The major limitations on the use of PANI and its composites in clinical practice include cytotoxicity, processability, the notable differences between *in vitro* and *in vivo* research, and physicochemical characteristics. PANI has poor processability, infusibility, and low solubility or insolubility in the most widely used solvents. However, PANI's poor physical characteristics and lack of biocompatibility pose the biggest obstacles to its tissue engineering applications, particularly for applications inside the human body, such as bone regeneration. The synthesis of PANI composites with nanostructures like Ag and TiO_2 and biodegradable synthetic polymers like PCL, poly(lactic-*co*-glycolic acid) PLGA, and poly(lactic acid) PLA has somewhat resolved this problem by enhancing their mechanical characteristics and ability to integrate into biological tissues. Furthermore, the biodegradability of pure PANI scaffolds continues to limit their use in tissue regeneration. Although the use of metallic nanoparticles improves the antibacterial effectiveness, some studies fail to sufficiently address concerns about cytotoxicity toward mammalian cells. Therefore, the development of degradable PANI blends and composites using biobased polymers has received a lot of attention.

As a next-generation material platform for efficient and sustainable biomedical solutions, PANI has significant potential; however, establishing its safety characteristics requires significant *in vivo* research and biocompatibility evaluations. The development of PANI-based biointerfaces for wearable and implantable devices will continue to be accelerated by developments in flexible electronics, nanofabrication, and 3D printing. PANI and its composites hold great promise for use as next-generation materials in enhanced diagnostic platforms, regenerative treatments, and precision medicine, by connecting polymer science and biomedical engineering.

5. Conclusion

This review provides a thorough analysis of PANI and its composites, highlighting their benefits and characteristics, from their synthesis, structure, and physicochemical characteristics to their potential in a variety of biomedical applications. PANI and its composites have emerged as versatile and promising materials for a broad spectrum of biological applications due to their inherent conductivity, redox activity, ease of functionalization, and compatibility with diverse nanostructures. Advances in material design have significantly improved their antimicrobial, antioxidant, antituberculosis, anticancer, and antimalarial activities. By adding hetero-ring, nanoparticles, carbon nanomaterials, and natural polymers to PANI matrices, their stability and biocompatibility have been improved, and their potential for medical analysis has been enhanced.

Author contributions

Chetna Kumari: writing – original draft, investigation; Sapana Jadoun: writing – review & editing, analysis; and Nirmala Kumari Jangid: writing – review & editing, supervision, and conceptualization.

Conflicts of interest

The authors declare that they have no known competing financial interests or personal relationships that could have appeared to influence the work reported in this paper.

Data availability

No primary research results, software or code have been included and no new data were generated or analysed as part of this review.

Acknowledgements

The authors acknowledge Prof. Ina Aditya Shastri, Vice-Chancellor, Banasthali Vidyapith, Rajasthan, India, for providing all the necessary facilities for the successful accomplishment of the present work. Authors also acknowledge to all the publisher to give permission for reproduce the figures, schemes, tables *etc*., in the review.

References

1 M. Maruthapandi, A. Saravanan, A. Gupta, J. H. Luong and A. Gedanken, Antimicrobial activities of conducting polymers and their composites, *Macromol*, 2022, **2**(1), 78–99, DOI: 10.3390/macromol2010005.
2 A. N. Andriianova, Y. N. Biglova and A. G. Mustafin, Effect of structural factors on the physicochemical properties of functionalized polyanilines, *RSC Adv.*, 2020, **10**(13), 7468–7491, DOI: 10.1039/C9RA08644G.
3 E. N. Zare, P. Makvandi, B. Ashtari, F. Rossi, A. Motahari and G. Perale, Progress in conductive polyaniline-based nanocomposites for biomedical applications: a review, *J. Med. Chem.*, 2019, **63**(1), 1–22, DOI: 10.1021/acs.jmedchem.9b00803.

4 J. Ouyang, Application of intrinsically conducting polymers in flexible electronics, *SmartMat*, 2021, **2**(3), 263–285, DOI: 10.1002/smm2.1059.
5 G. Kaur, R. Adhikari, P. Cass, M. Bown and P. Gunatillake, Electrically conductive polymers and composites for biomedical applications, *RSC Adv.*, 2015, **5**(47), 37553–37567, DOI: 10.1039/C5RA01851J.
6 T. Sen, S. Mishra and N. G. Shimpi, Synthesis and sensing applications of polyaniline nanocomposites: a review, *RSC Adv.*, 2016, **6**(48), 42196–42222, DOI: 10.1039/C6RA03049A.
7 I. Fratoddi, I. Venditti, C. Cametti and M. V. Russo, Chemiresistive polyaniline-based gas sensors: A mini review, *Sens. Actuators, B*, 2015, **220**, 534–548, DOI: 10.1016/j.snb.2015.05.107.
8 F. Kazemi, S. M. Naghib, Y. Zare and K. Y. Rhee, Biosensing applications of polyaniline (PANI)-based nanocomposites: A review, *Polym. Rev.*, 2021, **61**(3), 553–597, DOI: 10.1080/15583724.2020.1858871.
9 A. H. Majeed, L. A. Mohammed, O. G. Hammoodi, S. Sehgal, M. A. Alheety, K. K. Saxena and N. U. Salmaan, A review on polyaniline: synthesis, properties, nanocomposites, and electrochemical applications, *Int. J. Polym. Sci.*, 2022, **2022**(1), 9047554, DOI: 10.1155/2022/9047554.
10 H. D. Kyomuhimbo and U. Feleni, Electroconductive green metal-polyaniline nanocomposites: synthesis and application in sensors, *Electroanalysis*, 2023, **35**(2), e202100636, DOI: 10.1002/elan.202100636.
11 P. L. Meena and A. K. Surela, Polyaniline based binary nanocomposite heterostructures with semiconductor photocatalysts for photocatalytic improvement, *J. Mol. Liq.*, 2024, **412**, 125828, DOI: 10.1016/j.molliq.2024.125828.
12 A. Boublia, Z. Guezzout, N. Haddaoui, M. Badawi, A. S. Darwish, T. Lemaoui and Y. Benguerba, The curious case of polyaniline-graphene nanocomposites: a review on their application as exceptionally conductive and gas sensitive materials, *Crit. Rev. Solid State Mater. Sci.*, 2024, **49**(5), 973–997, DOI: 10.1080/10408436.2023.2274900.
13 M. Zahid, R. Anum, S. Siddique, H. F. Shakir and Z. A. Rehan, Polyaniline-based nanocomposites for electromagnetic interference shielding applications: A review, *J. Thermoplast. Compos. Mater.*, 2023, **36**(4), 1717–1761, DOI: 10.1177/08927057211022408.
14 A. Rayar, C. S. Naveen, H. S. Onkarappa, V. S. Betageri and G. D. Prasanna, EMI shielding applications of PANI-Ferrite nanocomposite materials: A review, *Synth. Met.*, 2023, **295**, 117338, DOI: 10.1016/j.synthmet.2023.117338.
15 S. Upadhyay, B. A. Bhat, R. Tomar and A. A. Bhat, Development and performance of a PANI@ NiMnO3 nanocomposite for enhanced supercapacitors and photocatalytic applications, *ACS Appl. Bio Mater.*, 2024, **7**(11), 7256–7268, DOI: 10.1021/acsabm.4c00954.
16 M. Maruthapandi, A. Saravanan, J. H. Luong and A. Gedanken, Antimicrobial properties of polyaniline and polypyrrole decorated with zinc-doped copper oxide microparticles, *Polymers*, 2020, **12**(6), 1286, DOI: 10.3390/polym12061286.
17 S. Abirami and E. Kumar, A review on metal oxide-doped polyaniline nanocomposites, *J. Mater. Sci.*, 2024, **59**(31), 14141–14171, DOI: 10.1007/s10853-024-10020-z.
18 P. L. Meena and J. K. Saini, Synthesis of polymer-metal oxide (PANI/ZnO/MnO_2) ternary nanocomposite for effective removal of water pollutants, *Results Chem.*, 2023, **5**, 100764, DOI: 10.1016/j.rechem.2023.100764.
19 M. Oves, M. Shahadat, S. A. Ansari, M. Aslam and I. I. Ismail, Polyaniline nanocomposite materials for biosensor designing, *Electrically Conductive Polymer and Polymer Composites: From Synthesis to Biomedical Applications*, 2018, pp. 113–135, DOI: 10.1002/9783527807918.ch6.
20 S. T. Jamil and B. I. Al-Abdaly, Polyaniline/metal oxide nanocomposites: synthesis, characterization and study of their applications, *Iraqi J. Sci.*, 2025, 4029–4044.
21 A. Jose, P. Yadav, D. Svirskis, S. Swift and M. R. Gizdavic-Nikolaidis, Antimicrobial photocatalytic PANI based-composites for biomedical applications, *Synth. Met.*, 2024, **303**, 117562, DOI: 10.1016/j.synthmet.2024.117562.
22 C. Wu, L. Shen, Y. Lu, C. Hu, Z. Liang, L. Long and Y. Wang, Intrinsic antibacterial and conductive hydrogels based on the distinct bactericidal effect of polyaniline for infected chronic wound healing, *ACS Appl. Mater. Interfaces*, 2021, **13**(44), 52308–52320, DOI: 10.1021/acsami.1c14088.
23 H. A. R. Abdullah, M. Q. Fahem, Z. T. Turki and M. H. Jawad, Effect of photothermal therapy using PANI-Fe_2O_3-Cys nanocomposites on breast cancer cells with antibacterial activity and cytotoxicity study, *Eur. Phys. J. E:Soft Matter Biol. Phys.*, 2025, **48**(6), 1–11, DOI: 10.1140/epje/s10189-025-00507-1.
24 M. R. Gizdavic-Nikolaidis, A. Jose, D. R. Stanisavljev, M. Marinović-Cincović, D. Marinković, D. Svirskis and S. Swift, Enhanced antimicrobial activity of photocatalytic titanium oxide upon formation of composites with polyaniline via an eco-friendly and facile microwave synthesis approach, *Ceram. Int.*, 2024, **50**(20), 38943–38951, DOI: 10.1016/j.ceramint.2024.07.258.
25 B. A. Shah, A. Sardar, W. Peng, S. T. U. Din, S. Hamayoun, S. Li and B. Yuan, Photoresponsive CuS@ polyaniline nanocomposites: An excellent synthetic bactericide against several multidrug-resistant pathogenic strains, *Inorg. Chem. Front.*, 2023, **10**(21), 6339–6356, DOI: 10.1039/D3QI01316B.
26 Y. Sohail, N. Raza, N. Shakeel, H. Raza, S. Manzoor, G. Yasmin and S. Mohammad Wabaidur, Polyaniline-coated nanoparticles of zinc oxide and copper oxide as antifungal agents against Aspergillus parasiticus, *Front. Plant Sci.*, 2022, **13**, 925451, DOI: 10.3389/fpls.2022.925451.
27 S. Manzoor, G. Yasmin, N. Raza, J. Fernandez, R. Atiq, S. Chohan and M. Azam, Synthesis of polyaniline coated magnesium and cobalt oxide nanoparticles through eco-friendly approach and their application as antifungal agents, *Polymers*, 2021, **13**(16), 2669, DOI: 10.3390/polym13162669.
28 N. Ahmad, S. Sultana, G. Kumar, M. Zuhaib, S. Sabir and M. Z. Khan, Polyaniline based hybrid bionanocomposites with enhanced visible light photocatalytic activity and

antifungal activity, *J. Environ. Chem. Eng.*, 2019, **7**(1), 102804, DOI: 10.1016/j.jece.2018.11.048.

29 C. Sridhar, N. Gunvanthrao Yernale and M. A. Prasad, Synthesis, spectral characterization, and antibacterial and antifungal studies of PANI/V_2O_5 nanocomposites, *Int. J. Chem. Eng.*, 2016, **2016**(1), 3479248, DOI: 10.1155/2016/3479248.

30 A. J. Ležaić, I. Pašti, A. Gledović, J. Antić-Stanković, D. Božić, S. Uskoković-Marković and G. Ćirić-Marjanović, Copolymerization of aniline and gallic acid: Novel electroactive materials with antioxidant and antimicrobial activities, *Synth. Met.*, 2022, **286**, 117048, DOI: 10.1016/j.synthmet.2022.117048.

31 M. Mecwan, N. Falcone, A. H. Najafabadi and D. Khorsandi, Antioxidant activity, *Electrically Conducting Polymers and Their Composites for Tissue Engineering*, American Chemical Society, 2023, pp. 71–80, DOI: 10.1021/bk-2023-1438.ch005.

32 J. P. Saikia, S. Banerjee, B. K. Konwar and A. Kumar, Biocompatible novel starch/polyaniline composites: characterization, anti-cytotoxicity and antioxidant activity, *Colloids Surf., B*, 2010, **81**(1), 158–164, DOI: 10.1016/j.colsurfb.2010.07.005.

33 A. Parsa and S. A. Salout, Investigation of the antioxidant activity of electrosynthesized polyaniline/reduced graphene oxide nanocomposite in a binary electrolyte system on ABTS and DPPH free radicals, *J. Electroanal. Chem.*, 2016, **760**, 113–118, DOI: 10.1016/j.jelechem.2015.11.021.

34 G. Kashyap, G. Ameta, C. Ameta, R. Ameta and P. B. Punjabi, Synthesis and characterization of polyaniline-drug conjugates as effective antituberculosis agents, *Bioorg. Med. Chem. Lett.*, 2019, **29**(11), 1363–1369, DOI: 10.1016/j.bmcl.2019.03.040.

35 J. Robertson, J. Dalton, S. Wiles, M. Gizdavic-Nikolaidis and S. Swift, The tuberculocidal activity of polyaniline and functionalised polyanilines, *PeerJ*, 2016, **4**, e2795, DOI: 10.7717/peerj.2795/supp-1.

36 D. Sudhadevi, P. Jayamurugan, G. Srinivas, B. Suresh, A. Gupta, R. Rajeshkumar and A. Kumar, An in vitro cytotoxicity study on PANI/ZnO nanocomposites against HCT-116 cancer cells using MTT assay, *Polym. Polym. Compos.*, 2024, **32**, 09673911241288320, DOI: 10.1177/09673911241288320.

37 B. Xia, B. Wang, J. Shi, Y. Zhang, Q. Zhang, Z. Chen and J. Li, Photothermal and biodegradable polyaniline/porous silicon hybrid nanocomposites as drug carriers for combined chemo-photothermal therapy of cancer, *Acta Biomater.*, 2017, **51**, 197–208, DOI: 10.1016/j.actbio.2017.01.015.

38 D. Sudhadevi, P. Jayamurugan, S. Deivanayaki, B. Yogeswari, B. Suresh, R. Rajeshkumar and G. Muteeb, The effect of TiO_2 concentration on the anticancer activity of PANI/TiO2 nanocomposites against HCT-116 cancer cell lines, *Polym. Bull.*, 2025, 1–24, DOI: 10.1007/s00289-025-05744-0.

39 T. Nezakati, A. Seifalian, A. Tan and A. M. Seifalian, Conductive polymers: opportunities and challenges in biomedical applications, *Chem. Rev.*, 2018, **118**(14), 6766–6843, DOI: 10.1021/acs.chemrev.6b00275.

40 S. Bhandari, Polyaniline: structure and properties relationship, *Polyaniline blends, composites, and nanocomposites*, Elsevier, 2018, pp. 23–60, DOI: 10.1016/B978-0-12-809551-5.00002-3.

41 N. Sharma, A. Singh, N. Kumar, A. Tiwari, M. Lal and S. Arya, A review on polyaniline and its composites: from synthesis to properties and progressive applications, *J. Mater. Sci.*, 2024, **59**(15), 6206–6244, DOI: 10.1007/s10853-024-09562-z.

42 H. Itoi, S. Hayashi, H. Matsufusa and Y. Ohzawa, Electrochemical synthesis of polyaniline in the micropores of activated carbon for high-performance electrochemical capacitors, *Chem. Commun.*, 2017, **53**(22), 3201–3204, DOI: 10.1039/C6CC08822H.

43 A. Gopalakrishnan and S. Badhulika, Three-dimensional $CoSe_2$ nanoparticles/PANI films composite via co-electrodeposition as a binder-free and a non-noble metal catalyst alternative for methanol oxidation application, *Mater. Chem. Phys.*, 2021, **273**, 125118, DOI: 10.1016/j.matchemphys.2021.125118.

44 T. V. Freitas, E. A. Sousa, G. C. Fuzari Jr and E. P. Arlindo, Different morphologies of polyaniline nanostructures synthesized by interfacial polymerization, *Mater. Lett.*, 2018, **224**, 42–45, DOI: 10.1016/j.matlet.2018.04.062.

45 A. N. Andriianova, R. B. Salikhov, L. R. Latypova, I. N. Mullagaliev, T. R. Salikhov and A. G. Mustafin, The structural factors affecting the sensory properties of polyaniline derivatives, *Sustainable Energy Fuels*, 2022, **6**(14), 3435–3445, DOI: 10.1039/D2SE00405D.

46 H. Peng, G. Ma, K. Sun, J. Mu, X. Zhou and Z. Lei, A novel fabrication of nitrogen-containing carbon nanospheres with high-rate capability as electrode materials for supercapacitors, *RSC Adv.*, 2015, **5**(16), 12034–12042, DOI: 10.1039/C4RA11889H.

47 N. K. Jangid, N. P. S. Chauhan, K. Meghwal, R. Ameta and P. B. Punjabi, Synthesis of dye-substituted polyanilines and study of their conducting and antimicrobial behavior, *Cogent Chem.*, 2015, **1**(1), 1084666, DOI: 10.1080/23312009.2015.1084666.

48 H. Cai, C. Feng, H. Xiao and B. Cheng, Synthesis of Fe_3O_4/rGO@ PANI with three-dimensional flower-like nanostructure and microwave absorption properties, *J. Alloys Compd.*, 2022, **893**, 162227, DOI: 10.1016/j.jallcom.2021.162227.

49 S. M. Naghib, Y. Zare and K. Y. Rhee, A facile and simple approach to synthesis and characterization of methacrylated graphene oxide nanostructured polyaniline nanocomposites, *Nanotechnol. Rev.*, 2020, **9**(1), 53–60.

50 B. Sim and H. J. Choi, Facile synthesis of polyaniline nanotubes and their enhanced stimuli-response under electric fields, *RSC Adv.*, 2015, **5**(16), 11905–11912, DOI: 10.1039/C4RA13635G.

51 C. Yin, L. Gao, F. Zhou and G. Duan, Facile synthesis of polyaniline nanotubes using self-assembly method based on the hydrogen bonding: Mechanism and application in

gas sensing, *Polymers*, 2017, **9**(10), 544, DOI: 10.3390/polym9100544.

52 C. D. Pina and E. Falletta, Advances in polyaniline for biomedical applications, *Curr. Med. Chem.*, 2022, **29**(2), 329–357, DOI: 10.2174/0929867328666210419135519.

53 S. Mandal, S. K. Saha and P. Chowdhury, Synthesis and characterization of polyaniline-based materials: their biological relevance-an overview, *Int. J. Curr. Microbiol. Appl. Sci.*, 2017, **6**, 2309–2321, DOI: 10.20546/ijcmas.2017.605.258.

54 A. J. Ležaić, I. Pašti, A. Gledović, J. Antić-Stanković, D. Božić, S. Uskoković-Marković and G. Ćirić-Marjanović, Copolymerization of aniline and gallic acid: Novel electroactive materials with antioxidant and antimicrobial activities, *Synth. Met.*, 2022, **286**, 117048, DOI: 10.1016/j.synthmet.2022.117048.

55 J. J. Jebarshia, T. Preethi, S. Ashokan, N. Geetha and K. Senthil, Co-doped polyaniline composites for biological application: Morphological, functional, optical and antibacterial activities, *Inorg. Chem. Commun.*, 2024, **161**, 111971, DOI: 10.1016/j.inoche.2023.111971.

56 M. R. Dos Santos, J. J. Alcaraz-Espinoza, M. M. da Costa and H. P. de Oliveira, Usnic acid-loaded polyaniline/polyurethane foam wound dressing: preparation and bactericidal activity, *Mater. Sci. Eng., C*, 2018, **89**, 33–40, DOI: 10.1016/j.msec.2018.03.019.

57 C. Dhivya, S. A. A. Vandarkuzhali and N. Radha, Antimicrobial activities of nanostructured polyanilines doped with aromatic nitro compounds, *Arabian J. Chem.*, 2019, **12**(8), 3785–3798, DOI: 10.1016/j.arabjc.2015.12.005.

58 K. Skopalová, I. N. Bubanja, D. Stanisavljev, N. Cvjetićanin, V. Kašpárková, E. Daďová and P. Humpolíček, The effect of synthesis method and oxidizing agent on cytotoxicity and ecotoxicity of polyaniline, *Synth. Met.*, 2024, **301**, 117515, DOI: 10.1016/j.synthmet.2023.117515.

59 C. Kumari, A. Singh, N. K. Jangid, J. Dwivedi and S. Sharma, Molecular docking and antibacterial activity of a one-pot synthesized novel polyaniline substituted imidazole (PANI–imidazole) copolymer, *New J. Chem.*, 2025, **49**(11), 4658–4667, DOI: 10.1039/D4NJ04331F.

60 P. Chaubisa, D. Dharmendra, Y. Vyas, P. Chundawat, C. Paliwal and C. Ameta, Biological activity of PANI–tetrazole and PANI–pyrazole composites against microbial strains, *Discover Chem.*, 2025, **2**(1), 1–13, DOI: 10.1007/s44371-025-00127-w.

61 C. Kumari, G. Kumar, S. Jadoun and N. K. Jangid, Impact of pyrazine doping on the electrical conductance and antimicrobial behaviour of novel one-pot synthesized polyaniline-*co*-pyrazine: DFT and molecular docking, *J. Mater. Chem. B*, 2025, **13**(39), 12640–12652, DOI: 10.1039/D5TB01302J.

62 P. Chaubisa, D. Dharmendra, Y. Vyas, P. Chundawat, N. K. Jangid and C. Ameta, Synthesis and characterization of PANI and PANI-indole copolymer and study of their antimalarial and antituberculosis activity, *Polym. Bull.*, 2024, **81**(4), 3333–3353, DOI: 10.1007/s00289-023-04873-8.

63 A. N. Andriianova, L. R. Latypova, L. Y. Vasilova, S. V. Kiseleva, V. V. Zorin, I. B. Abdrakhmanov and A. G. Mustafin, Antibacterial properties of polyaniline derivatives, *J. Appl. Polym. Sci.*, 2021, **138**(47), 51397, DOI: 10.1002/app.51397.

64 W. Cai, J. Wang, X. Quan and Z. Wang, Preparation of bromo-substituted polyaniline with excellent antibacterial activity, *J. Appl. Polym. Sci.*, 2018, **135**(1), 45657.

65 X. Quan, J. Wang, T. Souleyman, W. Cai, S. Zhao and Z. Wang, Antibacterial and antifouling performance of bisphenol-A/Poly (ethylene glycol) binary epoxy coatings containing bromine-benzyl-disubstituted polyaniline, *Prog. Org. Coat.*, 2018, **124**, 61–70, DOI: 10.1016/j.porgcoat.2018.08.010.

66 J. Kalaiarasi, D. Balakrishnan, L. A. Al-Keridis, F. A. Almekhlafi, M. A. Farrag, C. C. Kanisha and C. Pragathiswaran, Sensing and antimicrobial activity of polyaniline doped with TiO_2 nanocomposite synthesis and characterization, *J. King Saud Univ., Sci.*, 2022, **34**(3), 101824, DOI: 10.1016/j.jksus.2022.101824.

67 S. P. Deshmukh, A. G. Dhodamani, S. M. Patil, S. B. Mullani, K. V. More and S. D. Delekar, Interfacially interactive ternary silver-supported polyaniline/multiwalled carbon nanotube nanocomposites for catalytic and antibacterial activity, *ACS Omega*, 2019, **5**(1), 219–227, DOI: 10.1021/acsomega.9b02526.

68 A. Ali, S. Chowdhury, M. A. Carr, A. V. Janorkar, M. Marquart, J. A. Griggs and M. D. Roach, Antibacterial and biocompatible polyaniline-doped titanium oxide layers, *J. Biomed. Mater. Res., Part B*, 2023, **111**(5), 1100–1111, DOI: 10.1002/jbm.b.35217.

69 M. Maruthapandi, A. Saravanan, J. H. Luong and A. Gedanken, Antimicrobial properties of the polyaniline composites against Pseudomonas aeruginosa and *Klebsiella pneumoniae*, *J. Funct. Biomater.*, 2020, **11**(3), 59, DOI: 10.3390/jfb11030059.

70 J. Alam, A. K. Shukla, M. A. Ansari, F. A. A. Ali and M. Alhoshan, Dye separation and antibacterial activities of polyaniline thin film-coated poly (phenyl sulfone) membranes, *Membranes*, 2020, **11**(1), 25, DOI: 10.3390/membranes11010025.

71 M. Maruthapandi, A. Saravanan, P. Manohar, J. H. Luong and A. Gedanken, Photocatalytic degradation of organic dyes and antimicrobial activities by polyaniline-nitrogen-doped carbon dot nanocomposite, *Nanomaterials*, 2021, **11**(5), 1128, DOI: 10.3390/nano11051128.

72 S. Falak, B. K. Shin and D. S. Huh, Antibacterial activity of polyaniline coated in the patterned film depending on the surface morphology and acidic dopant, *Nanomaterials*, 2022, **12**(7), 1085, DOI: 10.3390/nano12071085.

73 K. Charoensri, C. Rodwihok, D. Wongratanaphisan, J. A. Ko, J. S. Chung and H. J. Park, Investigation of functionalized surface charges of thermoplastic starch/zinc oxide nanocomposite films using polyaniline: The potential of improved antibacterial properties, *Polymers*, 2021, **13**(3), 425, DOI: 10.3390/polym13030425.

74 Y. Hou, J. Feng, Y. Wang and L. Li, Enhanced antibacterial activity of Ag-doped ZnO/polyaniline nanocomposites, *J. Mater. Sci.: Mater. Electron.*, 2016, **27**(7), 6615–6622, DOI: 10.1007/s10854-016-4669-0.

75 H. Zengin, G. Aksin, G. Zengin, M. Kahraman and I. H. Kilic, Preparation and characterization of conductive polyaniline/silver nanocomposite films and their antimicrobial studies, *Polym. Eng. Sci.*, 2019, **59**(S1), E182–E194.

76 P. Boomi, G. P. Poorani, S. Palanisamy, S. Selvam, G. Ramanathan, S. Ravikumar and M. Saravanan, Evaluation of antibacterial and anticancer potential of polyaniline-bimetal nanocomposites synthesized from chemical reduction method, *J. Cluster Sci.*, 2019, **30**(3), 715–726, DOI: 10.1007/s10876-019-01530-x.

77 M. Shaban, M. Rabia, W. Fathallah, N. A. El-Mawgoud, A. Mahmoud, H. Hussien and O. Said, Preparation and characterization of polyaniline and Ag/polyaniline composite nanoporous particles and their antimicrobial activities, *J. Polym. Environ.*, 2018, **26**(2), 434–442, DOI: 10.1007/s10924-017-0937-1.

78 R. Bushra, M. Naushad, G. Sharma, A. Azam and Z. A. ALOthman, Synthesis of polyaniline based composite material and its analytical applications for the removal of highly toxic Hg^{2+} metal ion: antibacterial activity against *E. coli*, *Korean J. Chem. Eng.*, 2017, **34**(7), 1970–1979, DOI: 10.1007/s11814-017-0076-3.

79 S. M. Nezhad, A. Kousha, Y. Rajabi, E. N. Zare and S. Rahimi, NIR-responsive engineered colloidal polyaniline/ZnO/UiO-66-NH_2 nanoplatform: A multifunctional photothermal agent for precision therapy in breast cancer, *Alexandria Eng. J.*, 2025, **126**, 204–219, DOI: 10.1016/j.aej.2025.04.085.

80 S. Sampurnam, S. Muthamizh, A. Khusro, K. A. Varman and V. Narayanan, *In vitro* assessment on antibacterial, antioxidant, and anticancer traits of chemically synthesized polyaniline/ZrO_2–Ag nanohybrid, *Bionanoscience*, 2025, **15**(1), 68, DOI: 10.1007/s12668-024-01662-z.

81 U. Bogdanović, S. Dimitrijević, S. D. Škapin, M. Popović, Z. Rakočević, A. Leskovac and V. Vodnik, Copper-polyaniline nanocomposite: role of physicochemical properties on the antimicrobial activity and genotoxicity evaluation, *Mater. Sci. Eng., C*, 2018, **93**, 49–60, DOI: 10.1016/j.msec.2018.07.067.

82 T. J. Jayeoye, F. N. Eze, S. Singh, O. O. Olatunde, S. Benjakul and T. Rujiralai, Synthesis of gold nanoparticles/polyaniline boronic acid/sodium alginate aqueous nanocomposite based on chemical oxidative polymerization for biological applications, *Int. J. Biol. Macromol.*, 2021, **179**, 196–205.

83 S. Manzoor, G. Yasmin, N. Raza, J. Fernandez, R. Atiq, S. Chohan and M. Azam, Synthesis of polyaniline coated magnesium and cobalt oxide nanoparticles through eco-friendly approach and their application as antifungal agents, *Polymers*, 2021, **13**(16), 2669, DOI: 10.3390/polym13162669.

84 B. R. Pasela, A. P. Castillo, R. Simon, M. T. Pulido, H. Mana-Ay, M. R. Abiquibil and K. L. Taaca, Synthesis and characterization of acetic acid-doped polyaniline and polyaniline–chitosan composite, *Biomimetics*, 2019, **4**(1), 15, DOI: 10.3390/biomimetics4010015.

85 M. H. Abdel Rehim, M. A. Yassin, H. Zahran, S. Kamel, M. E. Moharam and G. Turky, Rational design of active packaging films based on polyaniline-coated polymethyl methacrylate/nanocellulose composites, *Polym. Bull.*, 2020, **77**(5), 2485–2499, DOI: 10.1007/s00289-019-02866-0.

86 M. R. Gizdavic-Nikolaidis, J. M. Pupe, A. Jose, L. P. Silva, D. R. Stanisavljev, D. Svirskis and S. Swift, Eco-friendly enhanced microwave synthesis of polyaniline/chitosan-AgNP composites, their physical characterisation and antibacterial properties, *Synth. Met.*, 2023, **293**, 117273, DOI: 10.1016/j.synthmet.2022.117273.

87 Y. Chen, Y. Li, Y. Yang, F. Wu, J. Cao and L. Bai, A polyaniline-reduced graphene oxide nanocomposite as a redox nanoprobe in a voltammetric DNA biosensor for *Mycobacterium tuberculosis*, *Microchim. Acta*, 2017, **184**(6), 1801–1808, DOI: 10.1007/s00604-017-2184-5.